Calhoun
Institutional Archive of the Naval Postgraduate School

Calhoun: The NPS Institutional Archive

DSpace Repository

Theses and Dissertations 1. Thesis and Dissertation Collection, all items

1971-06

Energy loss of high energy electrons in various metals: comparison of theory and experiments

Barry, William Francis; Oppedahl, Phillip Edward

http://hdl.handle.net/10945/15697

Downloaded from NPS Archive: Calhoun

DUDLEY KNOX LIBRARY

Calhoun is the Naval Postgraduate School's public access digital repository for research materials and institutional publications created by the NPS community. Calhoun is named for Professor of Mathematics Guy K. Calhoun, NPS's first appointed -- and published -- scholarly author.

Dudley Knox Library / Naval Postgraduate School
411 Dyer Road / 1 University Circle
Monterey, California USA 93943

http://www.nps.edu/library

ENERGY LOSS OF HIGH ENERGY ELECTRONS IN VARIOUS METALS: COMPARISON OF THEORY AND EXPERIMENT

William Francis Barry

United States
Naval Postgraduate School

THESIS

ENERGY LOSS OF HIGH ENERGY ELECTRONS IN VARIOUS METALS: COMPARISON OF THEORY AND EXPERIMENT

by

William Francis Barry

and

Phillip Edward Oppedahl

June 1971

Approved for public release; distribution unlimited.

T139782

Energy Loss of High Energy Electrons in Various Metals: Comparison of Theory and Experiment

by

William Francis Barry
Captain, United States Army
B.S., United States Military Academy, 1966

and

Phillip Edward Oppedahl
Commander, United States Navy
B.S., Naval Postgraduate School, 1963

Submitted in partial fulfillment of the
requirements for the degree of

MASTER OF SCIENCE IN PHYSICS

from the

NAVAL POSTGRADUATE SCHOOL
June 1971

Thesis
B2 [illegible] 3
c.1

ABSTRACT

A comparison of data from all previous energy loss experiments performed at the Naval Postgraduate School with new theoretical predictions is presented in this thesis. In addition, the data have been extended to include beryllium. With this extension, experiments have now been conducted on materials ranging in atomic number from 4 to 82. Agreement between experiment and theory is excellent for the most probable energy loss. However, theoretical values for the half-widths of the energy loss distributions generally are small compared to experiment for thicknesses less than 5 g/cm^2 and large for thicknesses greater than 5 g/cm^2. These experiments were conducted in the energy range from 50 to 100 MeV, with absorber thicknesses from 0.7 to 5.9 g/cm^2. These effects were found to be independent of atomic number or incident energy.

TABLE OF CONTENTS

I. INTRODUCTION ---------- 7

II. THEORETICAL CONSIDERATIONS ---------- 9

III. EXPERIMENTAL PROCEDURE ---------- 12

IV. TREATMENT OF DATA ---------- 15

V. RESULTS AND CONCLUSIONS ---------- 17

APPENDIX A Tables ---------- 21

APPENDIX B Figures ---------- 26

APPENDIX C Beam Folding Technique ---------- 52

APPENDIX D Computer Program ---------- 55

BIBLIOGRAPHY ---------- 68

INITIAL DISTRIBUTION LIST ---------- 69

FORM DD 1473 ---------- 70

LIST OF TABLES

I. ENERGY LOSS DISTRIBUTION CHARACTERISTICS OF BERYLLIUM ------- 21

II. ENERGY LOSS DISTRIBUTION CHARACTERISTICS OF ALUMINUM -------- 22

III. ENERGY LOSS DISTRIBUTION CHARACTERISTICS OF COPPER ---------- 23

IV. ENERGY LOSS DISTRIBUTION CHARACTERISTICS OF TIN ------------- 24

V. ENERGY LOSS DISTRIBUTION CHARACTERISTICS OF GADOLINIUM ----- 24

VI. ENERGY LOSS DISTRIBUTION CHARACTERISTICS OF LEAD ----------- 25

LIST OF FIGURES

1. Experimental Arrangement -- 12

2. Trend Plot of HW_{exp}/HW_{th} vs Absorber Thickness ----------------- 18

3. Comparison of Experimental and Theoretical Half-widths vs Absorber Thickness -- 18

4. Most Probable Energy Loss vs Beryllium Absorber Thickness ------ 26

5. Half-widths vs Beryllium Absorber Thickness ------------------- 27

6. Energy Distribution, Beryllium Absorber, $t = 0.742$ g/cm^2 $E_i = 52.89$ MeV -------- 28

7. Energy Distribution, Beryllium Absorber, $t = 1.479$ g/cm^2 $E_i = 52.89$ MeV -------- 29

8. Energy Distribution, Beryllium Absorber, $t = 2.209$ g/cm^2 $E_i = 52.89$ MeV -------- 30

9. Energy Distribution, Beryllium Absorber, $t = 2.961$ g/cm^2 $E_i = 52.89$ MeV -------- 31

10. Energy Distribution, Beryllium Absorber, $t = 3.673$ g/cm^2 $E_i = 52.89$ MeV -------- 32

11. Energy Distribution, Beryllium Absorber, $t = 4.415$ g/cm^2 $E_i = 52.89$ MeV -------- 33

12. Energy Distribution, Beryllium Absorber, $t = 5.179$ g/cm^2 $E_i = 52.89$ MeV -------- 34

13. Energy Distribution, Beryllium Absorber, $t = 5.908$ g/cm^2 $E_i = 52.89$ MeV -------- 35

14. Energy Distribution, Beryllium Absorber, $t = 0.738$ g/cm^2 $E_i = 74.78$ MeV -------- 36

15. Energy Distribution, Beryllium Absorber, $t = 1.479$ g/cm^2 $E_i = 74.78$ MeV -------- 37

16. Energy Distribution, Beryllium Absorber, $t = 2.209$ g/cm^2 $E_i = 74.78$ MeV -------- 38

17. Energy Distribution, Beryllium Absorber, $t = 2.941$ g/cm^2 $E_i = 74.78$ MeV -------- 39

18. Energy Distribution, Beryllium Absorber, $t = 3.673$ g/cm^2
$E_i = 74.78$ MeV -------- 40

19. Energy Distribution, Beryllium Absorber, $t = 4.435$ g/cm^2
$E_i = 74.78$ MeV -------- 41

20. Energy Distribution, Beryllium Absorber, $t = 5.179$ g/cm^2
$E_i = 74.78$ MeV -------- 42

21. Energy Distribution, Beryllium Absorber, $t = 5.908$ g/cm^2
$E_i = 74.78$ MeV -------- 43

22. Energy Distribution, Beryllium Absorber, $t = 0.738$ g/cm^2
$E_i = 94.64$ MeV -------- 44

23. Energy Distribution, Beryllium Absorber, $t = 1.479$ g/cm^2
$E_i = 94.64$ MeV -------- 45

24. Energy Distribution, Beryllium Absorber, $t = 2.209$ g/cm^2
$E_i = 94.64$ MeV -------- 46

25. Energy Distribution, Beryllium Absorber, $t = 2.941$ g/cm^2
$E_i = 94.64$ MeV -------- 47

26. Energy Distribution, Beryllium Absorber, $t = 3.673$ g/cm^2
$E_i = 94.64$ MeV -------- 48

27. Energy Distribution, Beryllium Absorber, $t = 4.435$ g/cm^2
$E_i = 94.64$ MeV -------- 49

28. Energy Distribution, Beryllium Absorber, $t = 5.179$ g/cm^2
$E_i = 94.64$ MeV -------- 50

29. Energy Distribution, Beryllium Absorber, $t = 5.908$ g/cm^2
$E_i = 94.64$ MeV -------- 51

30. Beam Folding Distributions ------------------------------------ 53

I. INTRODUCTION

Fast electrons which traverse a layer of material will exit with less energy than they possessed on entry. The energy loss distribution can be characterized by two parameters, the most probable energy loss (Q_p) and the half-width (HW), which is the full width at half maximum of the distribution curve. These quantities are the basis for comparison between experimental and theoretical results. Losses can be attributed to two major effects, ionization and radiation (bremsstrahlung). Ionization losses for fast electrons have been calculated by Landau [1], Williams [2], and many others. Early experiments resulted in good agreement with theory for the energy loss, but these results gave a half-width which was greater than theory at energies above 1 MeV. Blunck and Westphal [3] modified previous theoretical calculations by introducing radiation losses. This additional energy loss is superimposed on the ionization loss and results in a larger half-width and enhancement of the tail of the distribution. Other losses have been discounted as unimportant relative to ionization and radiation. All of the theoretical calculations are limited to "thin" absorbers, i.e., those in which Q_p is small compared to the incident electron energy.

Several measurements of energy loss for high energy electrons through various materials have been conducted at the Naval Postgraduate School. All were performed within an energy range of 50 to 100 MeV. These include the works of Bumiller, Buskirk, Dyer, and Miller on aluminum [4,5]; Goodwin on aluminum and copper [6]; DeLeuil, Raynis, et al on

aluminum, copper, and lead [7,8]; and Mosbrooker and Sandquist on tin, lead, and gadolinium [9]. With the extension to beryllium, data are now available on various materials with atomic numbers (Z) between 4 and 82.

Experimental consistency with past experiments was insured by rerunning several thicknesses of lead absorbers. Numerous and extensive checks were made on the computer program (Appendix D) written by Mosbrooker and Sandquist [9] to insure that it was consistent with Blunck and Westphal [3] theory as modified by the beam folding technique (Appendix C) which accounts for the energy spread of the incident beam.

Comparison of all experimental data taken at the Naval Postgraduate School with the theoretical results of Blunck and Westphal [3] is presented in this thesis. The data on beryllium are entirely new; the older data have been presented before, but the theoretical values given here are new and represent calculations made with the computer program of Appendix D.

II. THEORETICAL CONSIDERATIONS

The Blunck and Westphal theory of the distribution for the energy loss of a beam of monoenergetic electrons in passing through a layer of absorbing material assumes that the energy loss Q is small compared to the initial beam energy, E_i. Let W(Q)dQ be the probability of energy loss between Q and Q + dQ, and X be that portion of the loss Q due to radiation. Hence, the ionization loss is Q - X. Considering these two loss processes, the probability of energy loss is

$$W(Q)dQ = \int_{o}^{Q} W_I(Q-X)W_S(X)dXdQ \qquad (1)$$

where W_I and W_S are the energy loss distributions for ionization and radiation respectively.

The Landau equation [1], as modified by Blunck and Leisegang [10], is used for the energy loss distribution due to ionization. The distribution is expressed as a function of Landau's dimensionless parameter λ as follows:

$$W_I(Q)dQ = \Phi(\lambda)\ d\lambda = \sum_n \frac{C_n\gamma_n}{\sqrt{b^2 + \gamma_n^{\ 2}}} \exp\left[- \frac{(\lambda - \lambda_n)^2}{b^2 + \gamma_n^{\ 2}} \right] d\lambda \qquad (2)$$

$$\text{where } \lambda = \frac{Q-\overline{Q}}{aR} + \ln\left[\frac{E_i}{aR}\right] - 1.116 \qquad (3)$$

The terms used in equations (2) and (3) are defined as follows:

C_n, γ_n, and λ_n are constants given by Blunck and Leisegang [10] and are used to fit Landau's distribution to a sum of gaussian functions.

R is the absorber thickness in cm.

The quantity "a" is a function of the atomic number Z, the atomic weight A, and the density ρ of the absorber; and $\beta(=v/c)$ of the electrons:

$$a = \frac{0.154\ Z\ \rho}{A\ \beta^2}\quad \text{MeV/cm.} \tag{4}$$

The quantity b^2 is a correction to Landau's theory given by Blunck and Leisegang [10]:

$$b^2 = \frac{3.0}{aR} \sum_m \frac{I_m N_m}{Z} \ln \left[\frac{2\ E_i}{I_m(1 - \beta^2)} \right], \tag{5}$$

where the summation is over the ionization potentials of the atomic electrons, and N_m is the number of electrons with ionization potential I_m.

$\overline{Q}$ is the average energy loss due to ionization (no radiation) for electrons of incident energy E_i, and is given by Sternheimer [11,12,13] as follows:

$$\overline{Q} = \frac{A_s t}{\beta^2} \left[B + 0.43 + \ln E_i - \beta^2 - C - a_s(X_1 - \log_{10} p/mc)^{m_s} \right] \text{MeV} \tag{6}$$

where t is the thickness in g/cm^2, and the constants A_s, B, C, X_1, a_s, and m_s are parameters of the absorber material. These parameters for tin, lead, copper, beryllium, aluminum, and various other materials are listed in reference [13]. The parameters for gadolinium are not listed but were interpolated by Mosbrooker and Sanquist [9].

For W_s, the energy loss distribution due to radiation, Blunck and Westphal [3] give:

$$W_s(Q)dQ = B\alpha R(Q/E_i)^{\alpha R}\ \frac{dQ}{Q} \tag{7}$$

where

$$\alpha = 1.4 \times 10^{-3} \frac{\rho Z}{A} \left[4/3 \ln \frac{183}{Z^{1/3}} + 1/9 \right] \text{cm}^{-1} \qquad (8)$$

and B is a normalizing factor = $\frac{1}{\Gamma(\alpha R + 1)}$.

The distribution of total energy loss according to Blunck and Westphal is obtained by putting equations (7) and (2) into equation (1) and performing the required integration. The result is the energy loss distribution for a single electron of incident energy E_i. For comparison of theoretical and experimental values, this distribution function was used, with corrections to account for the finite energy width of the incident electron beam. This treatment is described in Section IV and Appendix C.

III. EXPERIMENTAL PROCEDURE

Beams of electrons ranging in energy from 53 to 95 MeV were obtained by using the LINAC of the Naval Postgraduate School. Electrons were elastically scattered from the accelerator beam through 90° by a thin (1 mil) aluminum foil. The electrons passed through the varying absorber thicknesses and were energy analyzed by a 120° magnetic spectrometer described by Kenaston, Luke and Sones [14].

The general experimental arrangement was similar to that used by Mosbrooker and Sandquist [9]. (See Figure 1). The energy of the incident electron beam was determined by using a nuclear magnetic resonance probe to measure the field of the deflection magnet of the LINAC. The scattered electrons are counted on a ten channel plastic scintillator counting system that consists of ten front counters and a single backing counter which is operated in coincidence with the front counters.

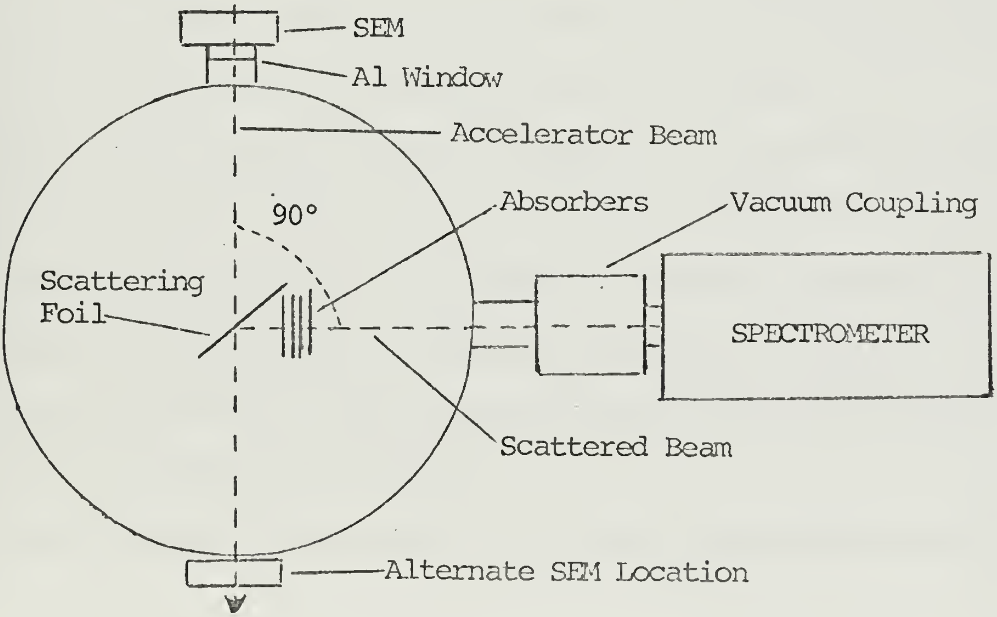

Figure 1. Experimental Arrangement

Beryllium absorbers of thicknesses ranging from 0.738 g/cm^2 to 5.908 g/cm^2 were mounted on a remotely controlled ladder that could be moved up and down vertically in the electron beam. This allowed us to collect data on one absorber thickness, then move the ladder and run a different thickness without having to enter the LINAC end station or change the LINAC beam in any way. The absorbers were placed at about 3 cm from the scattering foil.

A lead absorber of thickness 2.825 g/cm^2 was used to compare our experimental data with the results of Mosbrooker and Sandquist [9]. The results were in agreement within experimental accuracy.

Since the electron beam scattered into the absorbing material was not monoenergetic, the energy distribution was measured before and after passing through the absorbers. The zero thickness absorber distributions found by passing the beam only through the scattering foil had half widths ranging from 0.21 MeV to 0.46 MeV, or an energy resolution of about 0.45%. Following the measurement of these "zero peaks", the varying absorber thicknesses were moved into place and an energy distribution was determined for each absorber thickness.

Because of the limited quantity of beryllium available and space requirements in the target chamber, it was not possible to place all eight absorber thicknesses on one ladder. Therefore, each time the beam energy was changed or the ladder arrangement was changed, a new zero peak was measured. This accounted for the possibility that the character of the beam might change.

The data represent the number of scattered electrons detected by the coincidence counting system at the exit of the spectrometer as a function of the energy selected by the spectrometer.

Normalization was controlled by integrating the current from a Secondary Emission Monitor. This instrument was mounted both up and downstream of the targets. There proved to be no significant difference in the width of the zero peaks due to the position of the monitor. Each data set (ten points) represents a given integrated charge, i.e., a certain number of electrons passing through the scattering foil.

IV. TREATMENT OF DATA

The data for the experiment were taken with the ten channel counting system as described in Section III. To reduce the data, account must be taken of the characteristics of the counting system. These include the energy spread of the counters, which is about 0.3% between counters or 3% for the entire system. Accordingly, the energy seen by the individual counters must be determined and also correction must be made for the differing efficiencies of the scintillators and associated electronics. A computer program has been written which determines the correct relative counter energies and also corrects for counter efficiencies. Background corrections, which were quite small, were determined by periodically removing the scatterer and absorbers from the beam.

The reduced data were then plotted and from these plots the experimental most probable energy losses and distribution half-widths were measured. These results and their uncertainties can be found in Table I in Appendix A.

Since the scattered electron beam is not monoenergetic and the Blunck and Westphal theory is based on a monoenergetic incident beam, to compare theory and experiment the theoretical model must be modified. This modification is accomplished by representing the incident distribution as a histogram, each bin of which has a definite energy, and then unfolding this distribution into the theoretical calculations carried out by an IBM 360/67 computer. The unfolding technique is described in Appendix C and the computer program used is in Appendix D.

The computer program described in Appendix D also calculates the theoretical half-widths and most probable energy losses. The program normalizes the theoretical curve to the experimental data and plots both the theoretical curve and experimental data. These plots for beryllium are shown in Figures [3] through [26] in Appendix B. The measurable parameters were compared and the final results are tabulated in Appendix A.

The comparison of all data from all previous energy loss experiments performed at the Naval Postgraduate School LINAC was accomplished by normalizing each set of experimental data to the Blunck and Westphal theory as calculated by the computer program described in Appendix D. The comparison of the theory parameters so obtained to the experimental data can be found in Tables II through VI in Appendix A.

V. RESULTS AND CONCLUSIONS

The theoretical predictions and experimental results for the most probable energy losses and half-widths for beryllium can be found in Table I, Appendix A. Our theoretical predictions and the experimental results from previous theses completed at the Naval Postgraduate School for aluminum, copper, tin, gadolinium and lead can be found in Tables II through VI respectively in Appendix A. The theoretical data shown are for the Blunck and Westphal theory as modified by the beam folding technique. In all tables BW refers to Blunck and Westphal theory, Q_p represents the most probable energy loss, and HW is the distribution half-width. The column headed % represents the percentage by which theory exceeds experiment.

Agreement between the Blunck and Westphal theory and our experimental results is excellent for the most probable energy loss. The average difference between experiment and theory is less than 0.5%. However, agreement for half-width is good only for thicknesses less than 1 g/cm^2 and is fair for thicknesses between 4 to 6 g/cm^2. This result in half-width comparison is in contrast to previous results where it was concluded that the Blunck and Westphal theory predicts satisfactorily for thin targets where "thin" was defined as $t(Z)^{1/3} \lesssim 13.5$, where t is the absorber thickness (g/cm^2) and Z is the absorber atomic number.

The observed trend for HW (experimental) divided by HW (theoretical) as a function of t (absorber thickness) is plotted in Figure 2.

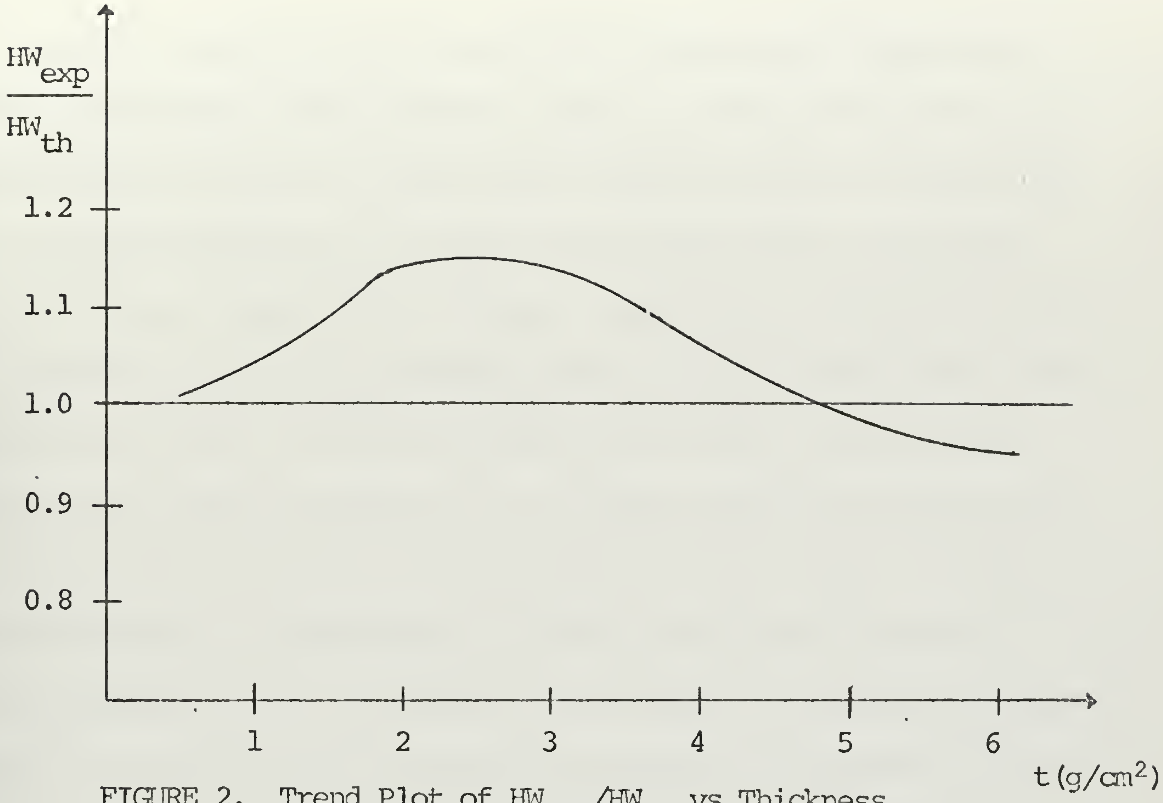

FIGURE 2. Trend Plot of HW_{exp}/HW_{th} vs Thickness

A typical comparison between experimental and theoretical curves for HW plotted as a function of t (absorber thickness) is presented in Figure 3.

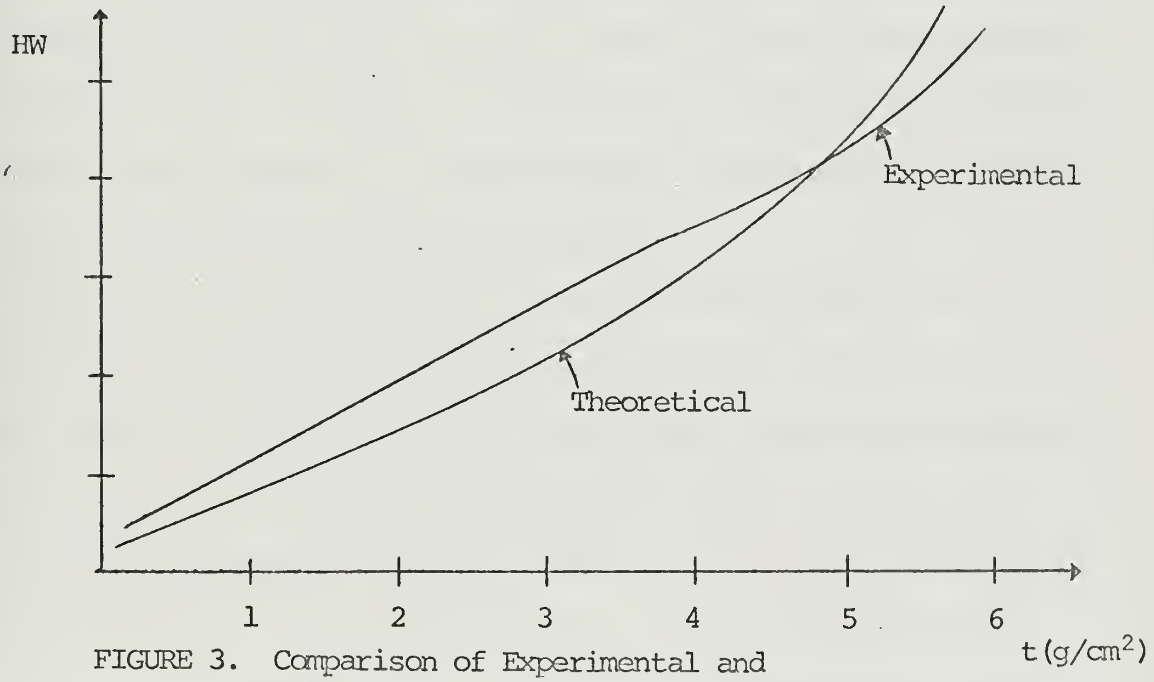

FIGURE 3. Comparison of Experimental and Theoretical Half-widths vs Thickness

As can be observed from these plots the theoretical half-width tends to be smaller than experiment until one gets to thick absorbers (approximately 5 g/cm^2) at which point it gets larger than experiment.

We have considered two possible effects which might explain why this crossing of experiment and theory takes place. One effect is that this trend is caused by an assumption that is made in the theory. This assumption is that of constant incident energy (E_i), i.e., that the energy loss is small compared to the incident energy of the electrons. However, in thick absorbers, this assumption is not valid, therefore the theory tends to overestimate the energy loss due to radiation (bremsstrahlung). This overestimate will cause an increase in the distribution tail and hence increase the distribution half-width. This trend in thick absorbers is not surprising in that the theory was originally designed for thin absorbers. The fact that the agreement is excellent for Q_p while not for half-width is also not surprising since an overestimate of this type would not affect the most probable energy loss significantly. Although this theoretical inaccuracy is undoubtedly a cause of some discrepancy in agreement with experiment, it is doubtful that it is the cause of all the disagreement.

The second possibility which we have considered affects the experimental results. Due to multiple scattering in thick absorbers the possibility existed that the size of the spectrometer opening was excluding the low energy portion of the distribution. However, calculations of the projected mean square scattering angle as outlined in Jackson [15] showed this angle to be approximately 0.30° while the spectrometer opening was approximately 0.90°. Therefore, it was determined that multiple scattering was not a factor in the disagreement of theory and experiment.

Discrepancies in the theoretical predictions from our program and previous results of Goodwin [6] and DeLeuil and Raynis [8] were noted. An attempt was made to resolve these differences. The parameters from Blunck and Westphal [3] were inserted into our computer program and without the unfolding technique described in Appendix C we were able to duplicate closely the Blunck and Westphal distributions. On this basis, it is assumed that our theoretical results are the more accurate.

Contrary to previous theses, the thickness at which theory and experiment began to exhibit a noticeable discrepancy was found not to be dependent on the atomic number of the material.

It should be mentioned that no attempt was made in this experiment to observe the very low energy tail of beryllium (approximately at 15 MeV) where in previous experiments secondary effects had caused a peak in the absorber distribution.

In light of what has been found in this thesis, further work is justified in several areas. First of all, the low energy tails of the various absorber distributions should be investigated to find out if secondary effects do cause a low energy peak in some distributions. Secondly, an effort should be made to improve the efficiency of the current computer program. Finally, an attempt should be made to extend the theory to thick absorbers where the energy loss is not small with respect to the incident energy, and also to include the effects of secondary processes.

APPENDIX A - TABLES

Table I. Energy Loss Distribution Characteristics of Beryllium

Be(Z = 4)		Q_p (MeV)			HW(MeV)		
E_i (MeV)	t(g/cm^2)	BW	Experimental	%	BW	Experimental	%
52.89	0.742	0.98	0.98 ± .02	-.30	0.33	0.36 ± .02	-8.3
	1.479	2.04	2.00 ± .04	+2.0	0.53	0.56 ± .04	-5.3
	2.209	3.05	2.96 ± .04	+3.0	0.67	0.77 ± .04	-13.0
	2.961	4.17	4.09 ± .08	+2.0	0.90	1.07 ± .07	-15.9
	3.673	5.29	5.19 ± .05	+2.0	1.17	1.25 ± .06	-6.4
	4.415	6.36	6.24 ± .13	+2.0	1.40	1.46 ± .09	-4.1
	5.179	7.46	7.40 ± .08	+.80	1.76	1.76 ± .10	0
	5.908	8.69	8.38 ± .12	+3.6	2.09	2.19 ± .14	-4.6
74.78	0.738	1.02	1.01 ± .03	-1.0	0.46	0.47 ± .04	-2.1
	1.479	2.04	2.01 ± .04	+1.5	0.56	0.61 ± .04	-8.2
	2.209	3.11	3.04 ± .05	+2.3	0.74	0.79 ± .05	-6.3
	2.941	4.15	4.15 ± .14	0	0.96	1.15 ± .08	-16.5
	3.673	5.29	5.15 ± .06	+2.7	1.17	1.39 ± .06	-15.8
	4.435	6.39	6.28 ± .10	+1.7	1.46	1.61 ± .10	-9.3
	5.179	7.46	7.42 ± .13	+.50	1.76	1.83 ± .08	-3.5
	5.908	8.68	8.51 ± .09	+2.0	2.12	2.24 ± .11	-5.3
94.64	0.738	1.02	1.05 ± .04	-2.7	0.58	0.57 ± .05	-1.7
	1.479	2.04	2.06 ± .04	-1.0	0.68	0.66 ± .04	+3.0
	2.209	3.11	3.09 ± .04	+.60	0.83	0.84 ± .06	-1.2
	2.941	4.15	4.06 ± .06	+2.7	1.06	1.22 ± .08	-13.1
	3.673	5.29	5.19 ± .06	+1.9	1.23	1.35 ± .08	-8.9
	4.435	6.39	6.30 ± .12	+1.4	1.53	1.58 ± .12	-3.2
	5.179	7.61	7.47 ± .12	+1.9	1.82	1.93 ± .10	-5.7
	5.908	8.69	8.63 ± .14	+.60	2.16	2.29 ± .11	-5.7

Table II. Energy Loss Distribution Characteristics of Aluminum

Al(Z = 14)		Q_p (MeV)			HW (MeV)		
E_i (MeV)	t (g/cm^2)	BW	Experimental	%	BW	Experimental	%
53.57	0.730	1.05	1.03	+1.9	0.44	0.49	-10.0
	1.441	2.12	2.16	-1.9	0.62	0.75	-17.0
	2.146	3.22	3.18	+1.2	0.88	1.02	-14.0
	2.859	4.29	4.21	+1.9	1.20	1.32	-9.1
53.44	5.574	8.86	9.24 ± .13	-4.1	3.12	4.60 ± .30	-32.0
74.63	0.730	1.05	1.04	+1.0	0.54	0.51	+5.9
	1.441	2.12	2.18	-2.7	0.72	0.91	-21.0
	2.146	3.22	3.17	+1.6	0.95	1.08	-12.0
	2.859	4.37	4.26	+2.6	1.25	1.38	-9.5
74.47	5.574	8.86	9.33 ± .25	-5.0	3.07	5.7 ± 1.2	-45.0
96.93	0.730	1.10	1.17	-6.0	0.64	0.66	-3.0
	1.441	2.16	2.16	-	0.81	1.01	-20.0
	2.146	3.22	3 24	-0.6	1.03	1.19	-13.0
	2.859	4.37	4.32	+1.2	1.31	1.48	-11.0

Table III. Energy Loss Distribution Characteristics of Copper

Cu(Z = 29)		Q_p (MeV)			HW(MeV)		
E_i (MeV)	t(g/cm^2)	BW	Experimental	%	BW	Experimental	%
52.84	0.711	0.92	0.94	-2.1	0.46	0.52	-12.0
	1.423	1.89	1.87	+1.1	0.69	0.84	-18.0
	2.134	2.90	2.87	+1.0	1.04	1.16	-10.0
	2.845	3.87	3.80	+1.8	1.54	1.75	-12.0
53.63	4.295	6.10	6.23 ± .13	-2.1	3.70	4.25 ± 1.20	-13.0
74.76	0.711	0.92	0.92	-	0.56	0.66	-15.0
	1.423	1.89	1.91	-1.0	0.78	1.07	-27.0
	2.134	2.90	2.92	-0.7	1.12	1.43	-22.0
	2.845	3.96	3.98	-0.5	1.61	1.98	-19.0
76.02	4.295	6.10	6.28 ± .13	-2.9	3.78	4.55 ± .50	-17.0
	5.726	8.65	8.38 ± .25	+3.2	10.37	10.1 ± 2.0	+3.6
94.30	0.711	0.91	0.95	-4.2	0.67	0.74	-9.5
	1.423	1.94	1.94	-	0.87	0.99	-12.0
	2.134	2.96	2.93	+1.0	1.22	1.47	-17.0
	2.845	3.99	4.00	-0.2	1.71	1.75	-2.3
96.66	5.726	8.82	9.20 ± .50	-4.1	10.50	16.4 ± 4.2	-37.0

Table IV. Energy Loss Distribution Characteristics of Tin

Sn(Z = 50)		Q_p (MeV)			HW(MeV)		
E_i (MeV)	t(g/cm^2)	BW	Experimental	%	BW	Experimental	%
52.53	1.485	1.83	1.78 ± .05	+2.8	0.75	0.78 ± .10	-3.8
	2.970	3.84	3.86 ± .15	-0.5	3.03	3.02 ± .40	+0.3
	4.455	6.56	6.35 ± .30	+3.3	16.70	11.30 ± 2.0	+48.0
75.00	1.485	1.81	1.77 ± .07	+9.0	0.73	0.83 ± .10	-12.0
	2.970	3.93	3.86 ± .15	+1.8	2.56	2.96 ± .42	-14.0
	4.455	6.56	6.65 ± .30	-1.4	16.69	15.50 ± 2.0	+7.7
94.40	1.485	1.88	1.87 ± .10	+0.5	0.83	0.88 ± .15	-5.7
	2.970	3.93	3.96 ± .20	-0.8	2.63	2.72 ± .45	-3.3
	4.455	6.56	7.00 ± 1.0	-6.3	16.75	16.20 ± 4.0	+3.4

Table V. Energy Loss Distribution Characteristics of Gadolinium

Gd(Z = 64)		Q_p (MeV)			HW(MeV)		
E_i (MeV)	t(g/cm^2)	BW	Experimental	%	BW	Experimental	%
53.18	0.814	0.97	0.92 ± .08	+5.4	0.46	0.52 ± .07	-12.0
52.80	1.610	1.94	1.92 ± .10	+1.0	0.91	1.00 ± .15	-8.9
	3.221	4.24	4.16 ± .30	+1.9	5.52	5.75 ± .72	-4.0
75.00	0.814	0.97	0.97 ± .05	-	0.51	0.59 ± .08	-13.0
	1.610	1.97	1.92 ± .10	+2.6	0.96	1.00 ± .15	-4.0
	3.221	4.24	4.09 ± .30	+3.7	5.55	5.80 ± .80	-4.2
91.80	0.814	0.97	0.97 ± .05	-	0.60	0.64 ± .08	-6.2
	1.610	1.97	1.90 ± .10	+3.7	0.96	1.10 ± .18	-13.0
	3.221	4.20	4.13 ± .40	+1.7	5.56	8.10 ± .95	-31.0

Table VI. Energy Loss Distribution Characteristics of Lead

Pb(Z = 82)		Q_p (MeV)			HW (MeV)		
E_i (MeV)	t (g/cm^2)	BW	Experimental	%	BW	Experimental	%
53.85	0.706	0.79	0.81 ± .05	-2.5	0.54	0.60 ± .06	-10.0
	1.412	1.66	1.45 ± .08	+14.0	0.97	1.23 ± .12	-21.0
	2.118	2.55	2.64 ± .10	-3.4	2.11	2.65 ± .25	-20.0
	2.825	3.57	3.66 ± .12*	-2.5	6.45	6.25 ± .50*	+3.2
74.74	0.706	0.83	0.82 ± .05	+1.2	0.78	0.82 ± .05	-4.9
	1.412	1.68	1.80 ± .10	-6.7	1.23	1.47 ± .07	-16.0
	2.118	2.66	2.59 ± .12	+2.7	2.37	2.24 ± .19	+5.8
	2.825	3.66	3.70 ± .15*	-1.1	6.52	6.25 ± .85*	+4.3
91.37	0.706	0.90	0.87 ± .07	+3.5	0.93	0.78 ± .08	+19.0
	1.412	1.80	1.77 ± .10	+1.7	1.37	1.52 ± .19	-9.8
	2.118	2.70	2.75 ± .15	-1.8	2.53	2.74 ± .64	-7.7
	2.825	3.69	3.84 ± .22	-3.9	6.95	8.80 ± .70	-22.0

*Experiment data average of DeLeuil/Raynis and Mosbrooker/Sandquist

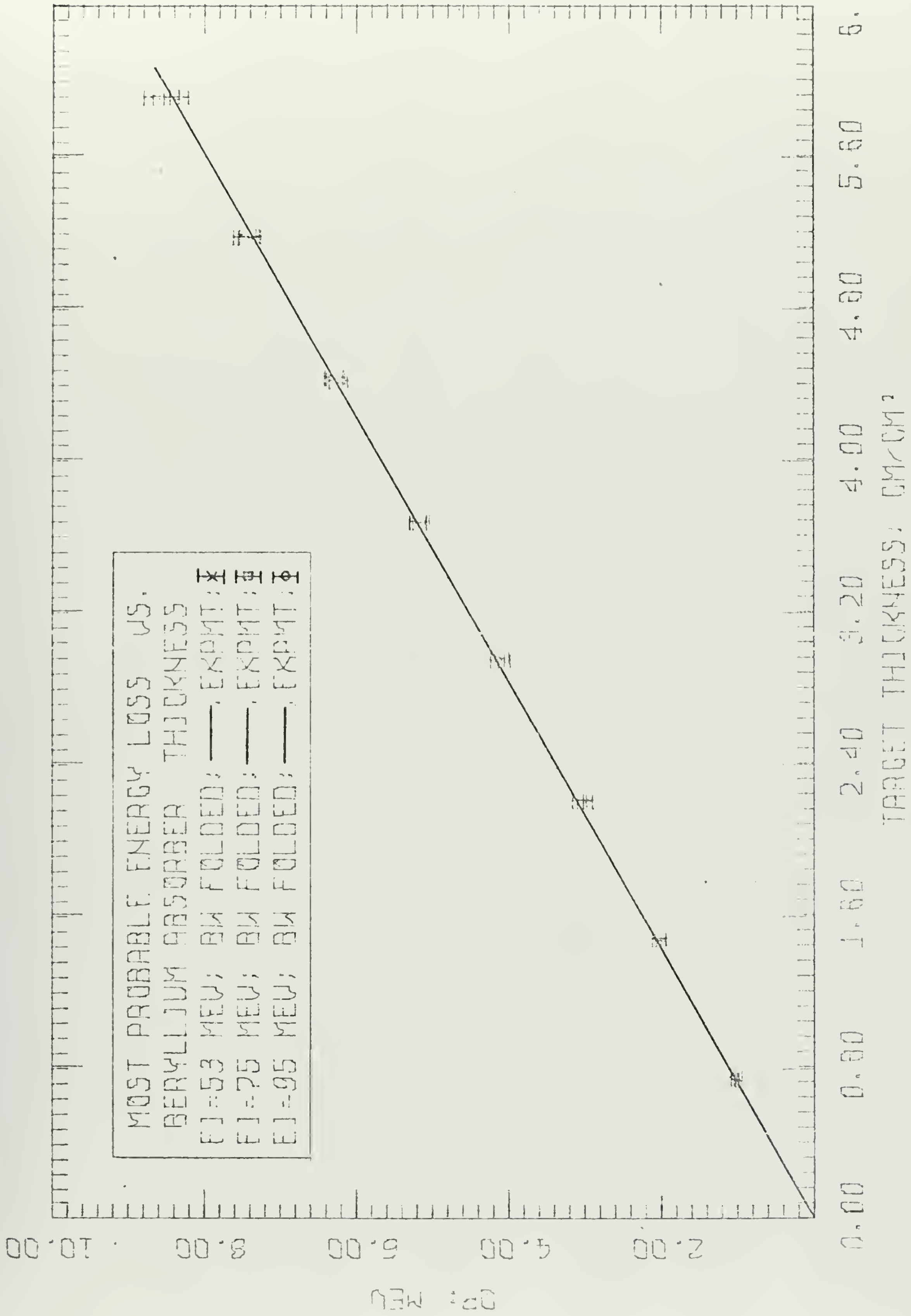
MOST PROBABLE ENERGY LOSS VS.
BERYLLIUM ABSORBER THICKNESS
EI=53 MEV; BW FOLDED; ——, EXPMT: ⌶
EI=75 MEV; BW FOLDED; ——, EXPMT: ⌶
EI=95 MEV; BW FOLDED; ——, EXPMT: ⌶
0.00
0.80
1.60
2.40
3.20
4.00
4.80
5.60
6.40
TARGET THICKNESS, GM/CM²
2.00
4.00
6.00
8.00
10.00
DE, MEV

Figure 4

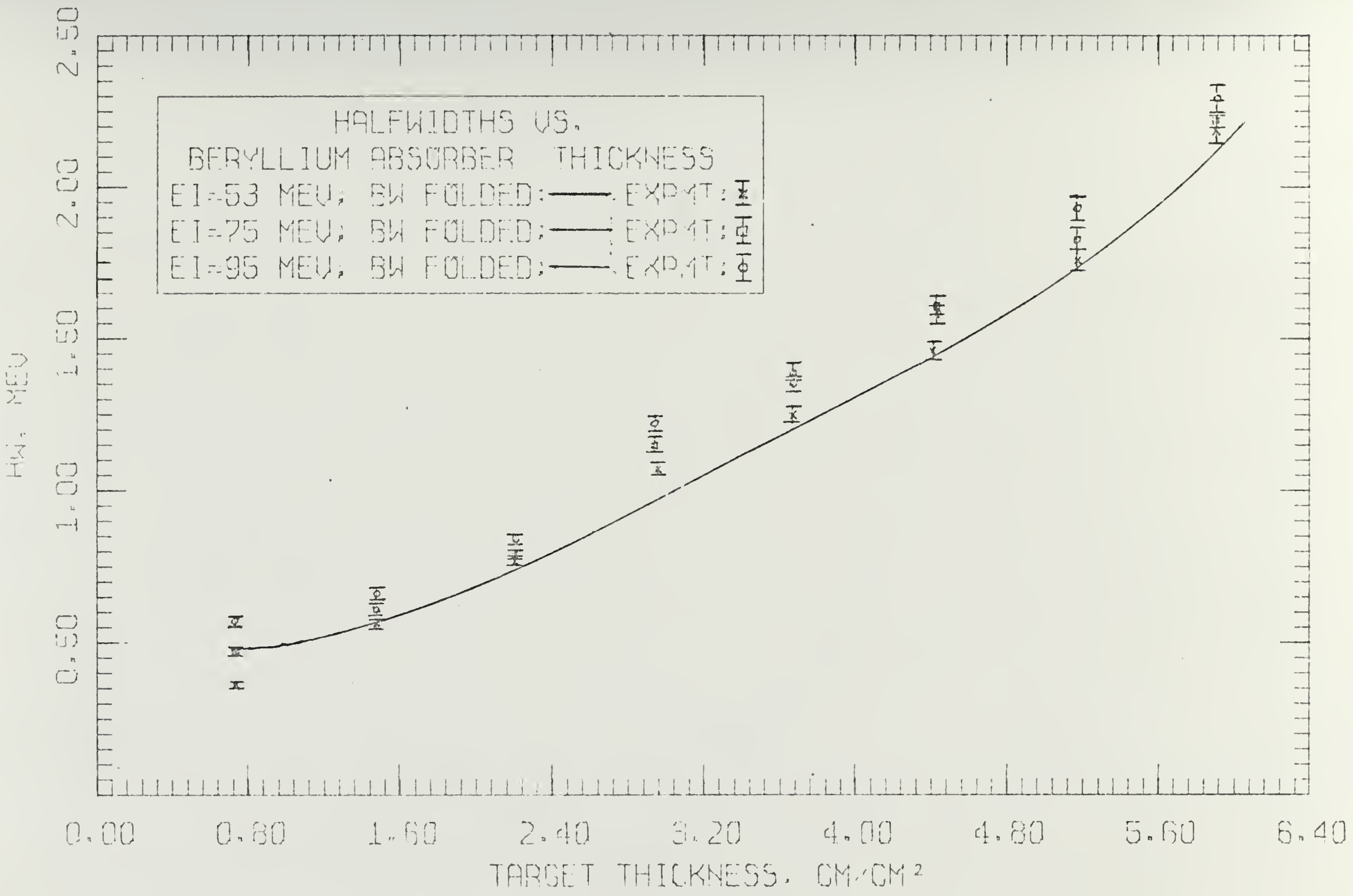
HALFWIDTHS VS.
BERYLLIUM ABSORBER THICKNESS
EI=53 MEV; BW FOLDED: EXP'T:
EI=75 MEV; BW FOLDED: EXP'T:
EI=95 MEV; BW FOLDED: EXP'T:
HW, MEV
0.50
1.00
1.50
2.00
2.50
0.00
0.80
1.60
2.40
3.20
4.00
4.80
5.60
6.40
TARGET THICKNESS, GM/CM²

Figure 5

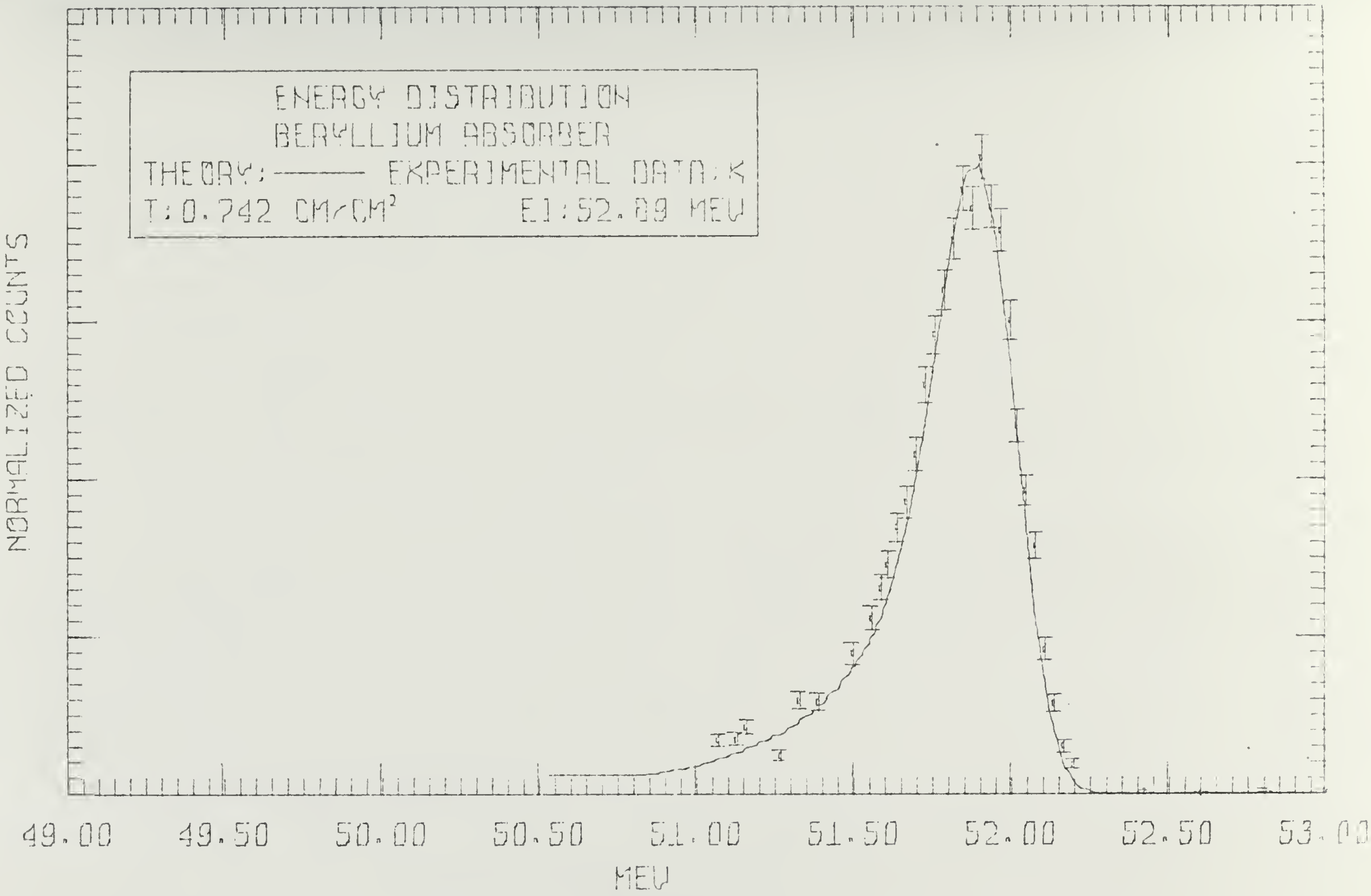
ENERGY DISTRIBUTION
BERYLLIUM ABSORBER
THEORY: ——— EXPERIMENTAL DATA: K
T: 0.742 CM/CM²
E1: 52.09 MEV
NORMALIZED COUNTS
49.00
49.50
50.00
50.50
51.00
51.50
52.00
52.50
53.00
MEV

Figure 6

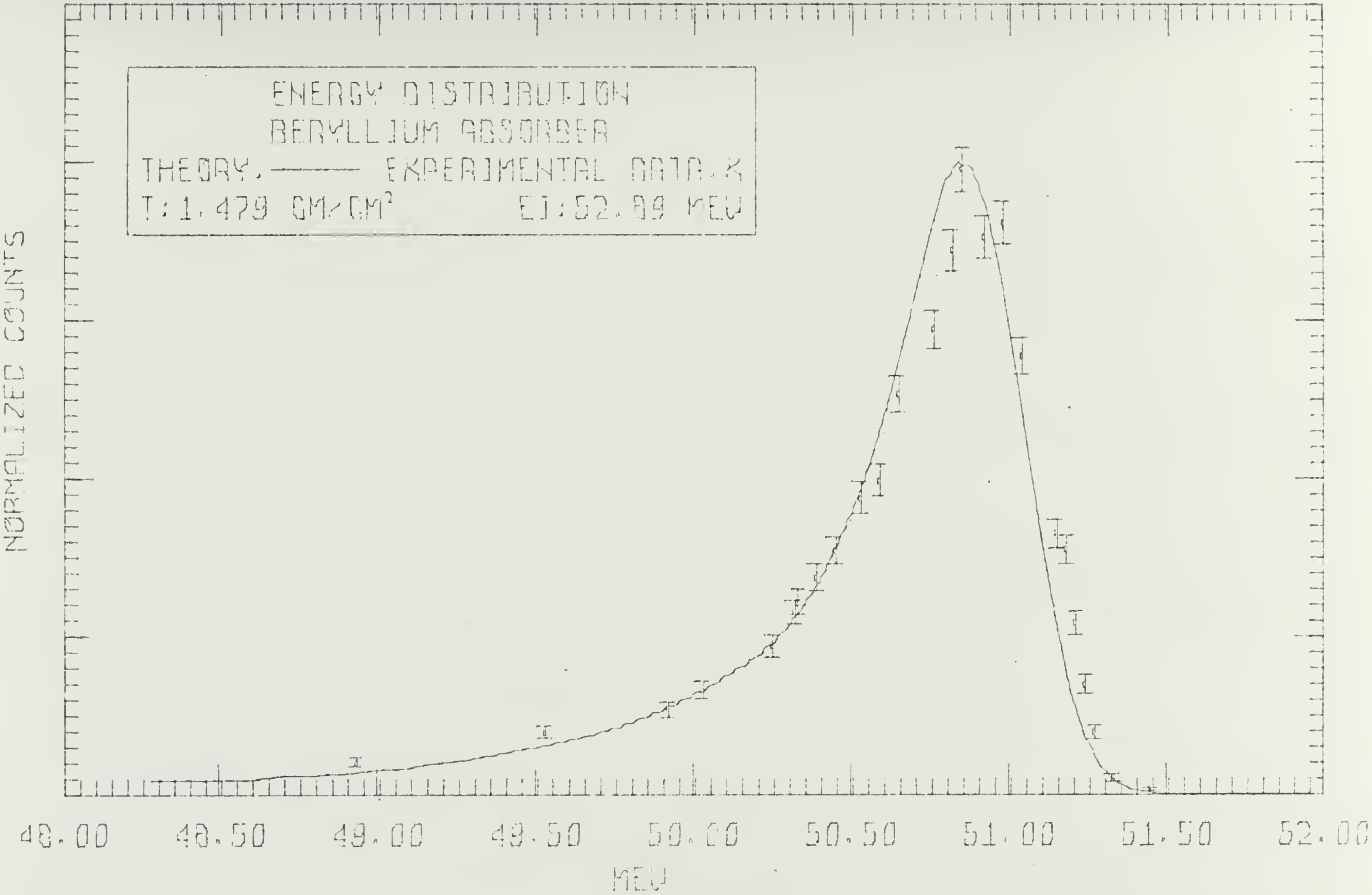
ENERGY DISTRIBUTION
BERYLLIUM ABSORBER
THEORY, ——— EXPERIMENTAL DATA, X
T: 1.479 GM/CM²
EI: 52.89 MEV
NORMALIZED COUNTS
48.00
48.50
49.00
49.50
50.00
50.50
51.00
51.50
52.00
MEV

Figure 7

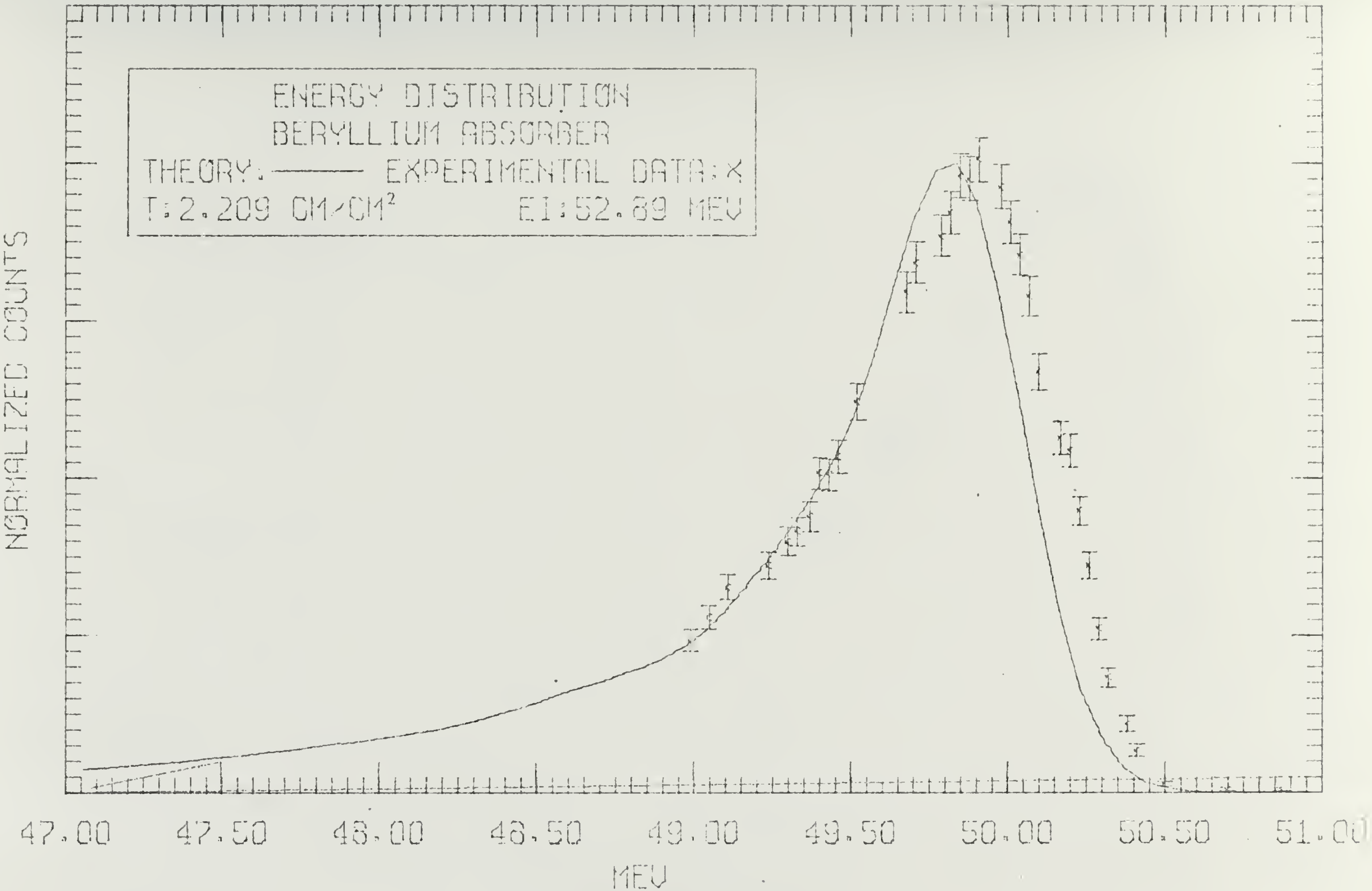
ENERGY DISTRIBUTION
BERYLLIUM ABSORBER
THEORY: ——— EXPERIMENTAL DATA: X
T: 2.209 GM/CM²
EI: 52.89 MEV
NORMALIZED COUNTS
47.00
47.50
48.00
48.50
49.00
49.50
50.00
50.50
51.00
MEV

Figure 8

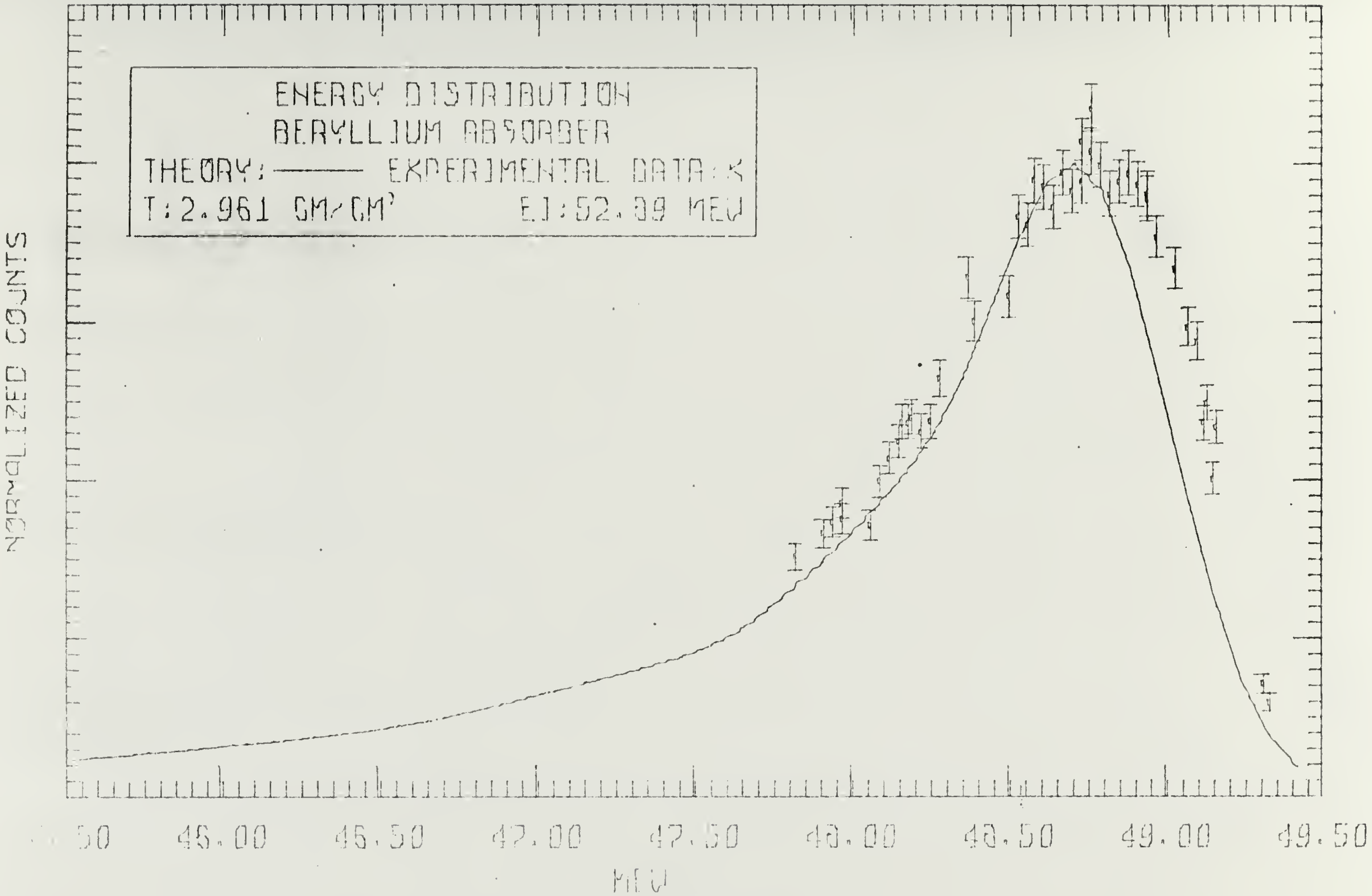
ENERGY DISTRIBUTION
BERYLLIUM ABSORBER
THEORY: ——— EXPERIMENTAL DATA: I
T: 2.961 GM/CM²
EI: 52.99 MEV
NORMALIZED COUNTS
50
46.00
46.50
47.00
47.50
48.00
48.50
49.00
49.50
MEV

Figure 9

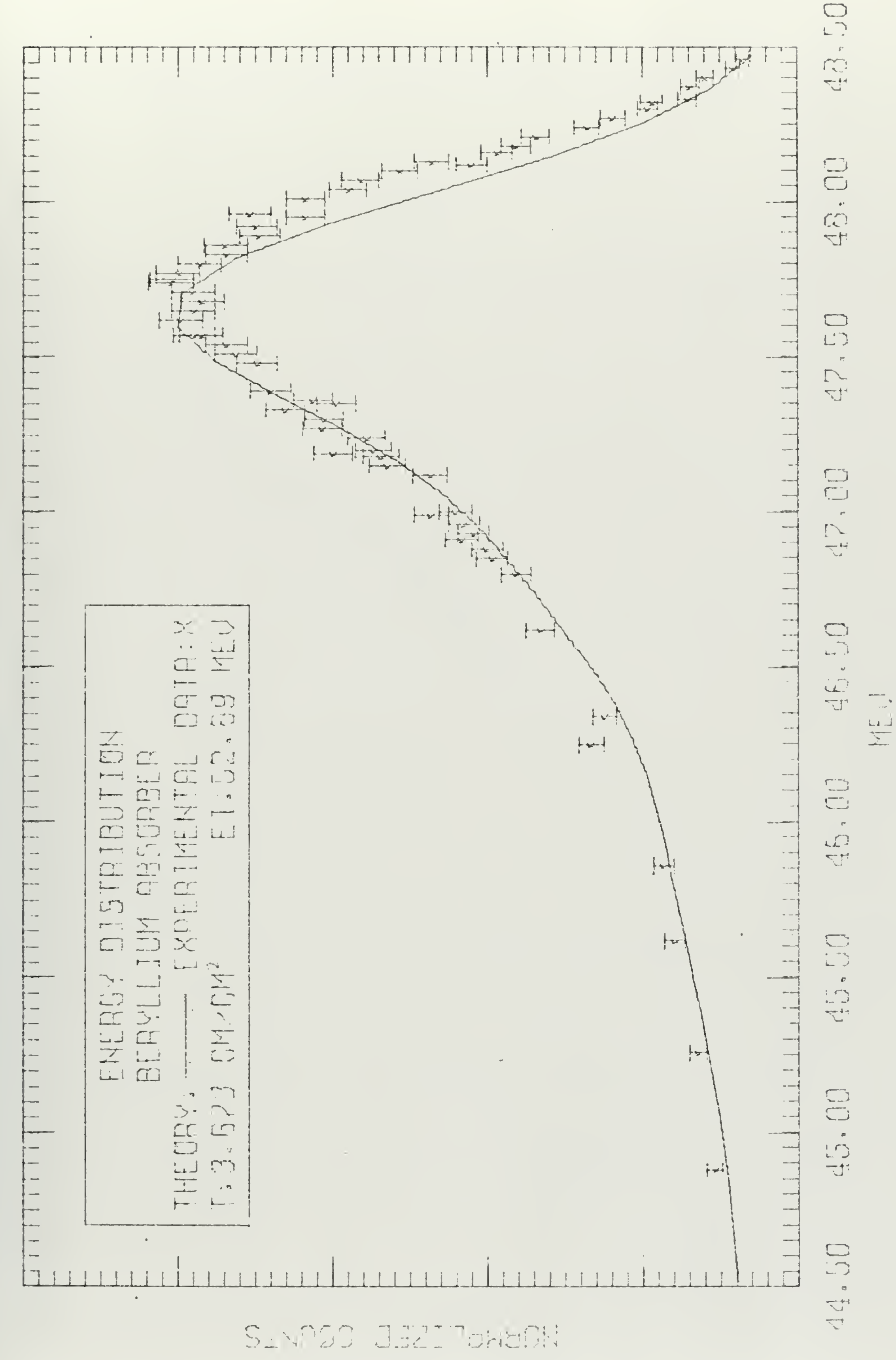
ENERGY DISTRIBUTION
BERYLLIUM ABSORBER
THEORY: —— EXPERIMENTAL DATA: X
T: 3.623 GM/CM²
E1: 52.89 MEV
NORMALIZED COUNTS
MEV
44.50
45.00
45.50
46.00
46.50
47.00
47.50
48.00
48.50

Figure 10

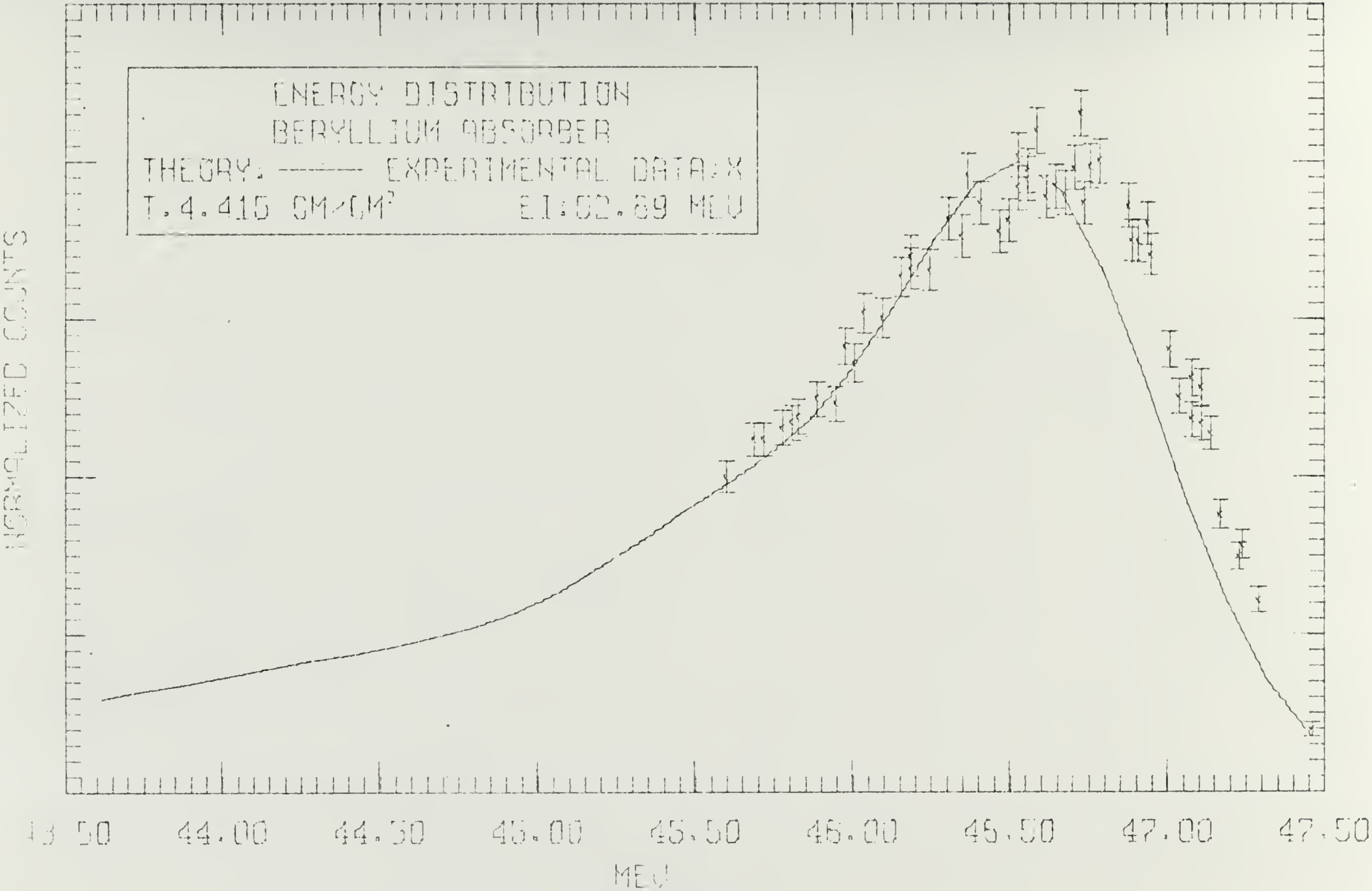
ENERGY DISTRIBUTION
BERYLLIUM ABSORBER
THEORY, ——— EXPERIMENTAL DATA:X
T,4.415 GM/CM²
EI:52.69 MEV
NORMALIZED COUNTS
43.50
44.00
44.50
45.00
45.50
46.00
46.50
47.00
47.50
MEV

Figure 11

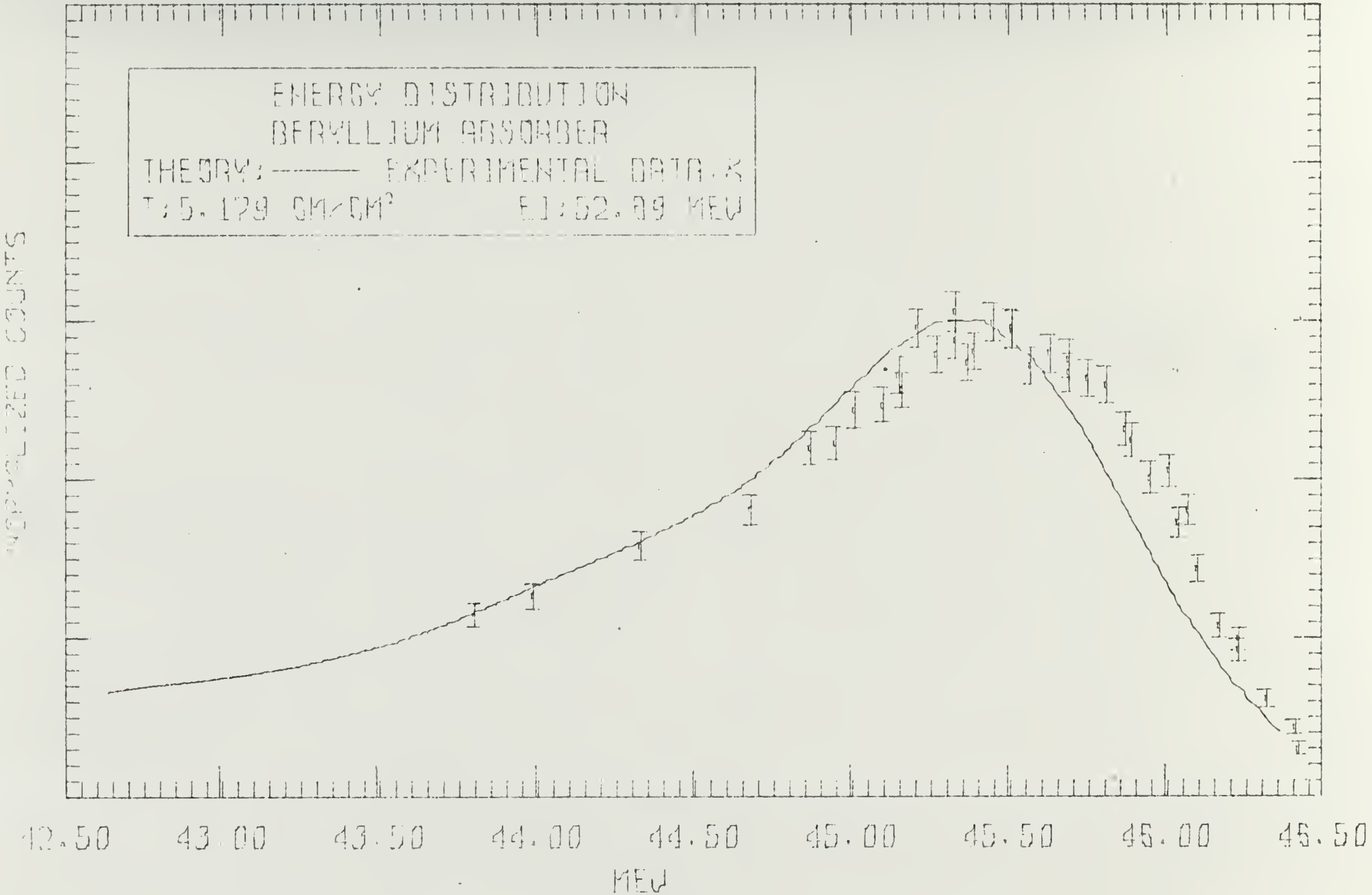
ENERGY DISTRIBUTION
BERYLLIUM ABSORBER
THEORY:——— EXPERIMENTAL DATA:X
T:5.129 GM/CM²
EI:52.09 MEV
NORMALIZED COUNTS
42.50
43.00
43.50
44.00
44.50
45.00
45.50
46.00
46.50
MEV

Figure 12

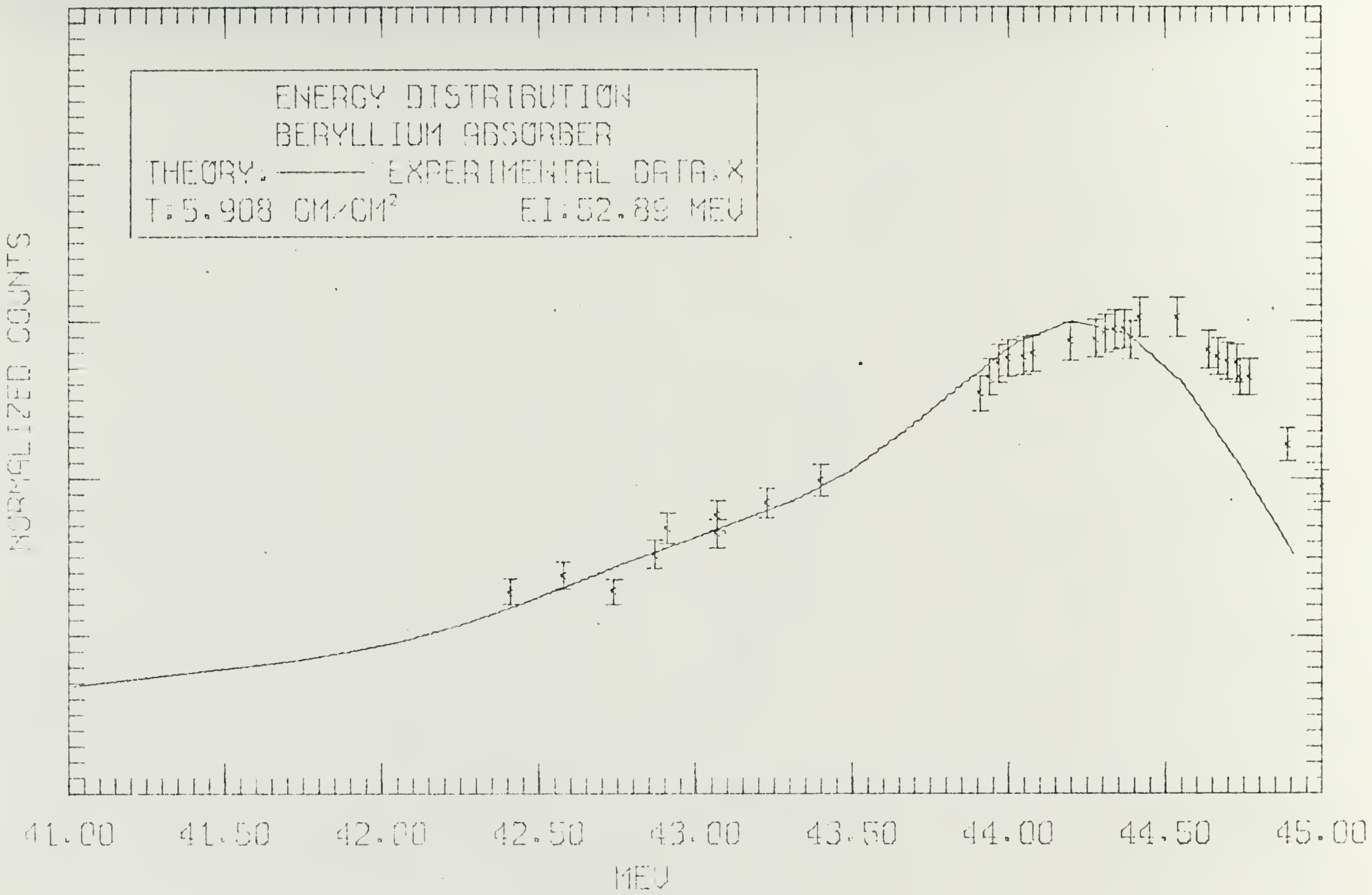
ENERGY DISTRIBUTION
BERYLLIUM ABSORBER
THEORY: —— EXPERIMENTAL DATA: X
T: 5.908 GM/CM^2
EI: 52.89 MEV
NORMALIZED COUNTS
41.00
41.50
42.00
42.50
43.00
43.50
44.00
44.50
45.00
MEV

Figure 13

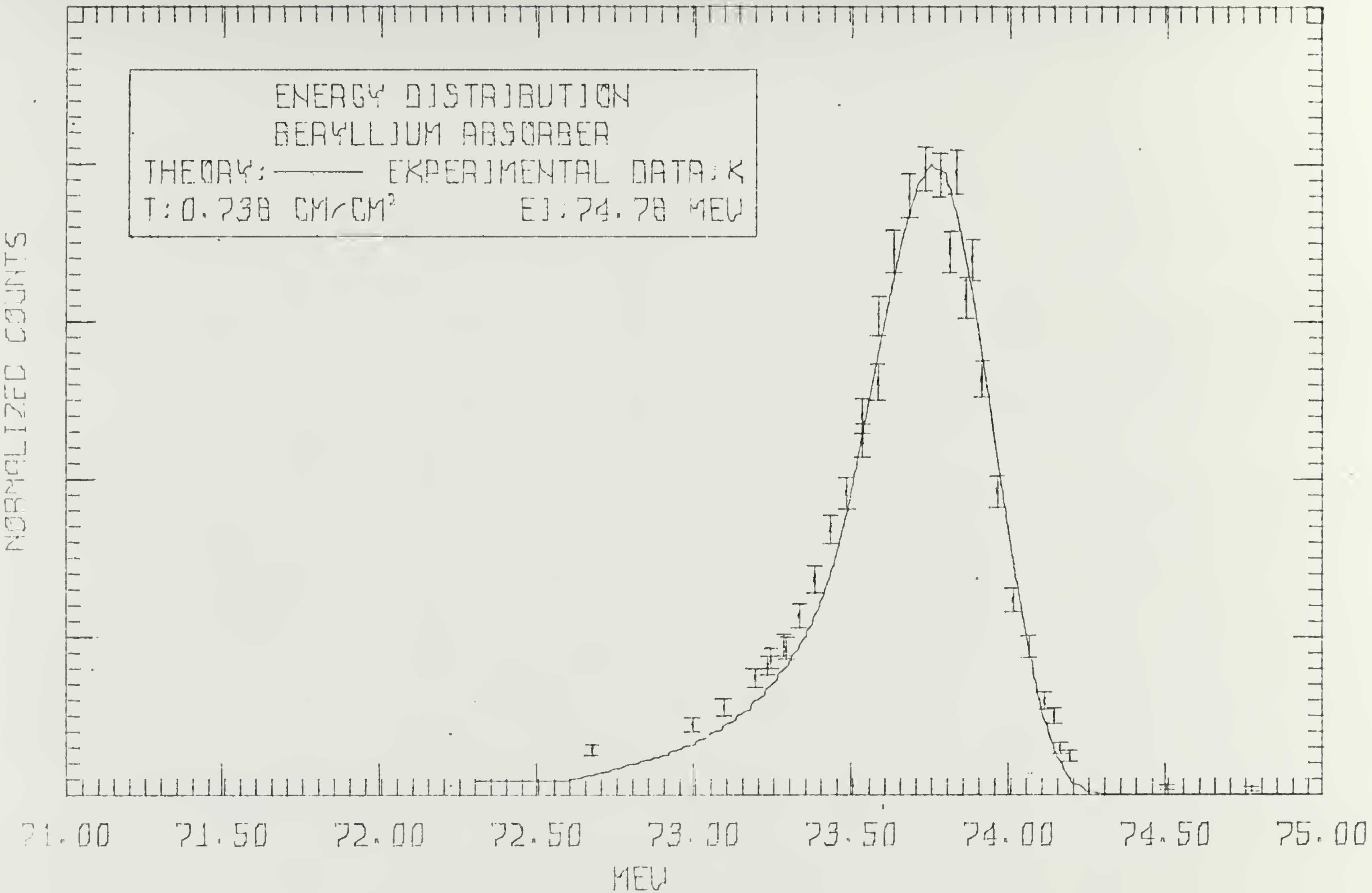
ENERGY DISTRIBUTION
BERYLLIUM ABSORBER
THEORY: ——— EXPERIMENTAL DATA:X
T:0.738 CM/CM²
EI:74.78 MEV
NORMALIZED COUNTS
21.00
21.50
22.00
22.50
23.00
23.50
24.00
24.50
25.00
MEV

Figure 14

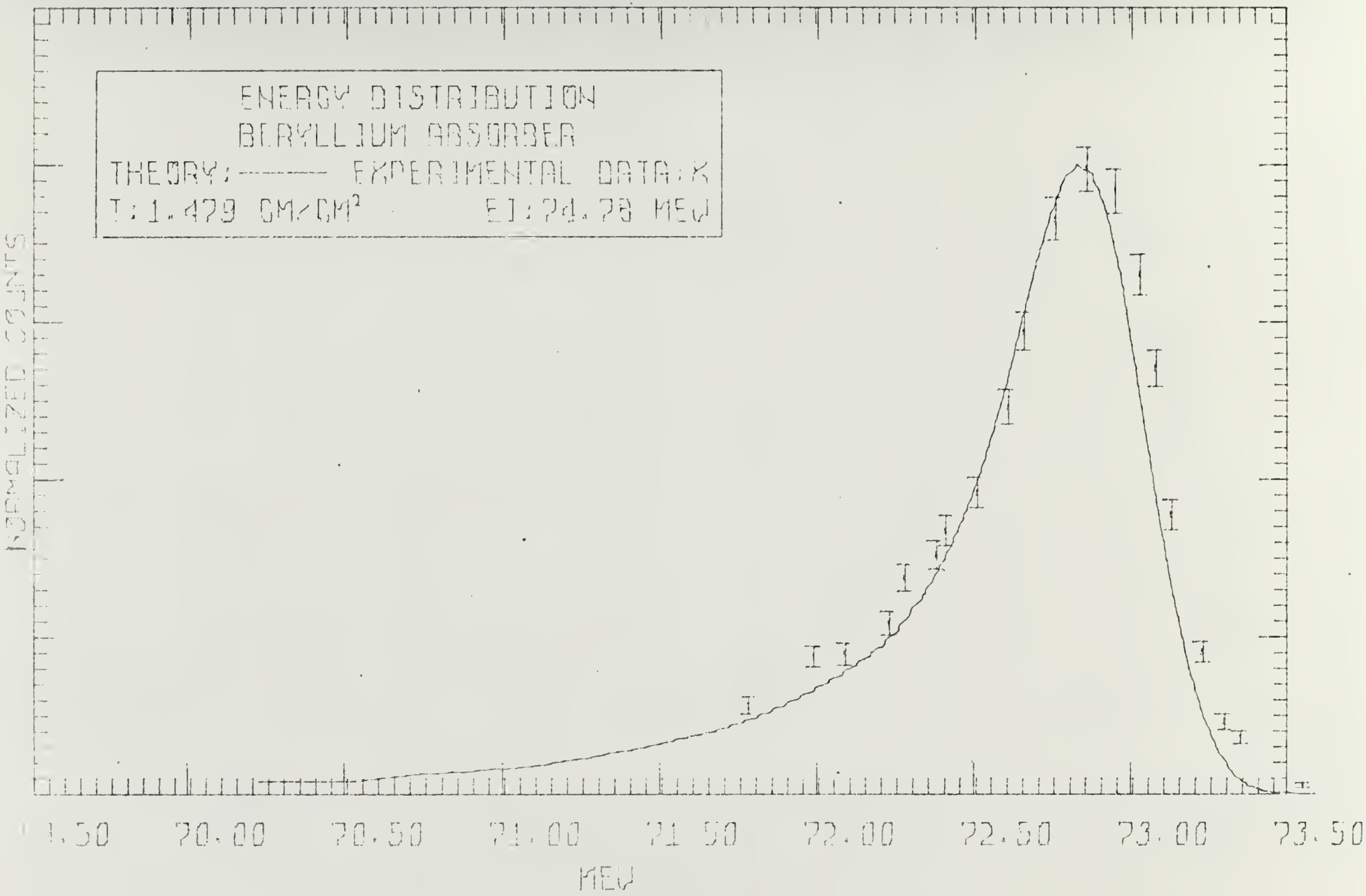
ENERGY DISTRIBUTION
BERYLLIUM ABSORBER
THEORY:——— EXPERIMENTAL DATA:K
T:1.479 GM/CM²
EI:74.78 MEV
NORMALIZED COUNTS
1.50
70.00
70.50
71.00
71.50
72.00
72.50
73.00
73.50
MEV

Figure 15

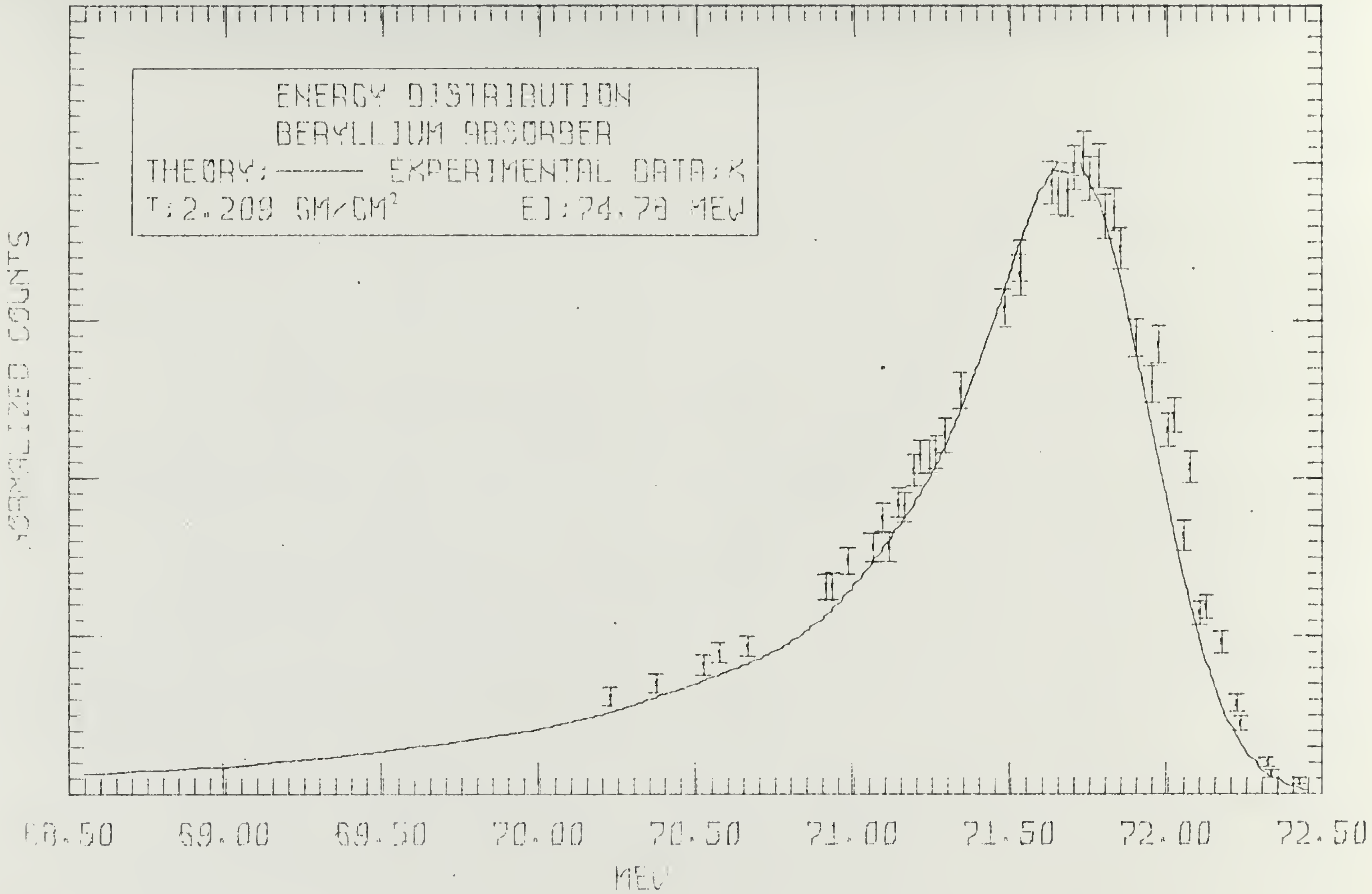
ENERGY DISTRIBUTION
BERYLLIUM ABSORBER
THEORY: ——— EXPERIMENTAL DATA: Ⅰ
T: 2.209 GM/CM²
EI: 74.79 MEV
NORMALIZED COUNTS
68.50
69.00
69.50
70.00
70.50
71.00
71.50
72.00
72.50
MEV

Figure 16

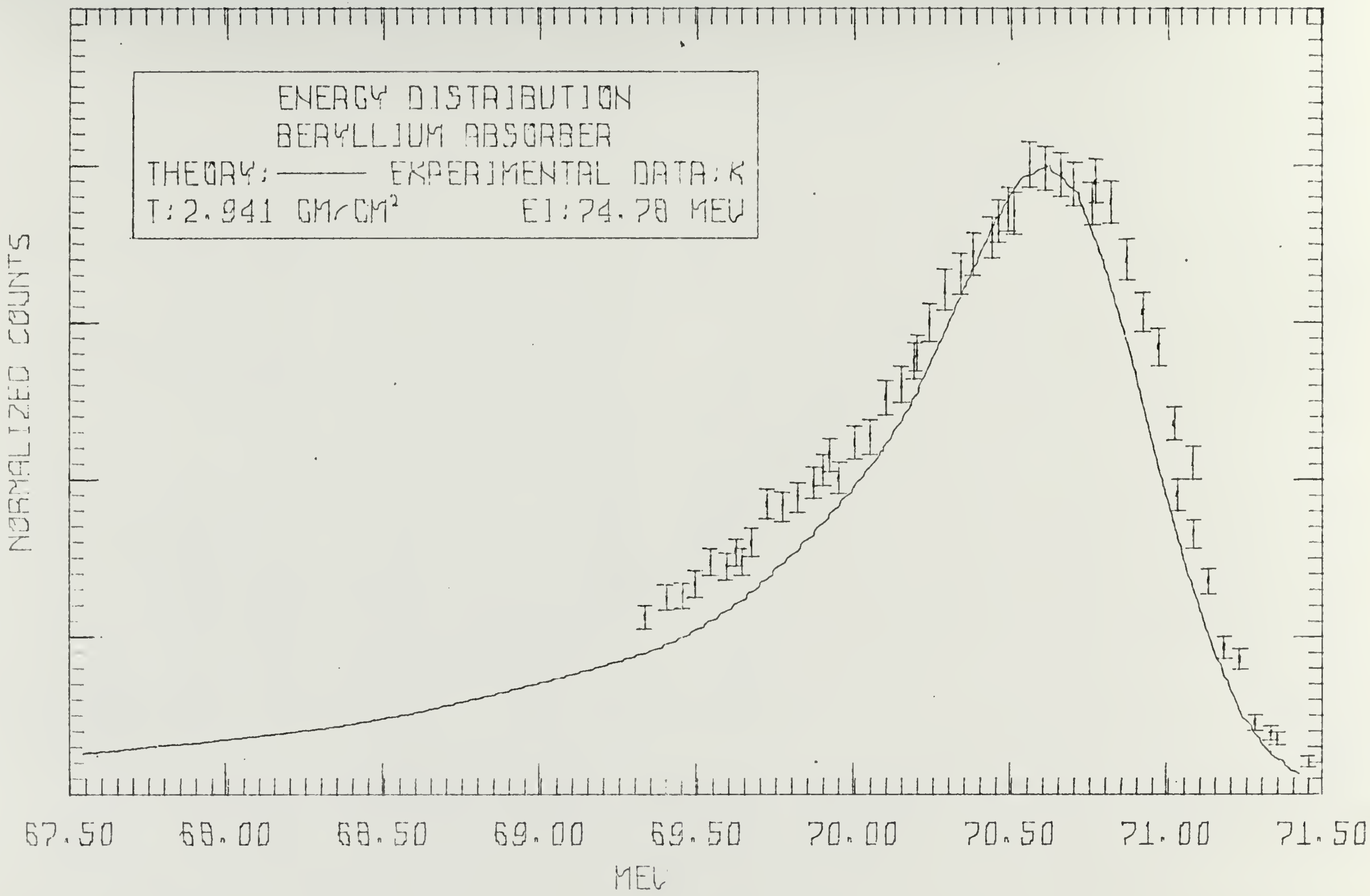
ENERGY DISTRIBUTION
BERYLLIUM ABSORBER
THEORY: ——— EXPERIMENTAL DATA: K
T: 2.941 GM/CM²
EI: 74.70 MEV
NORMALIZED COUNTS
67.50
68.00
68.50
69.00
69.50
70.00
70.50
71.00
71.50
MEV

Figure 17

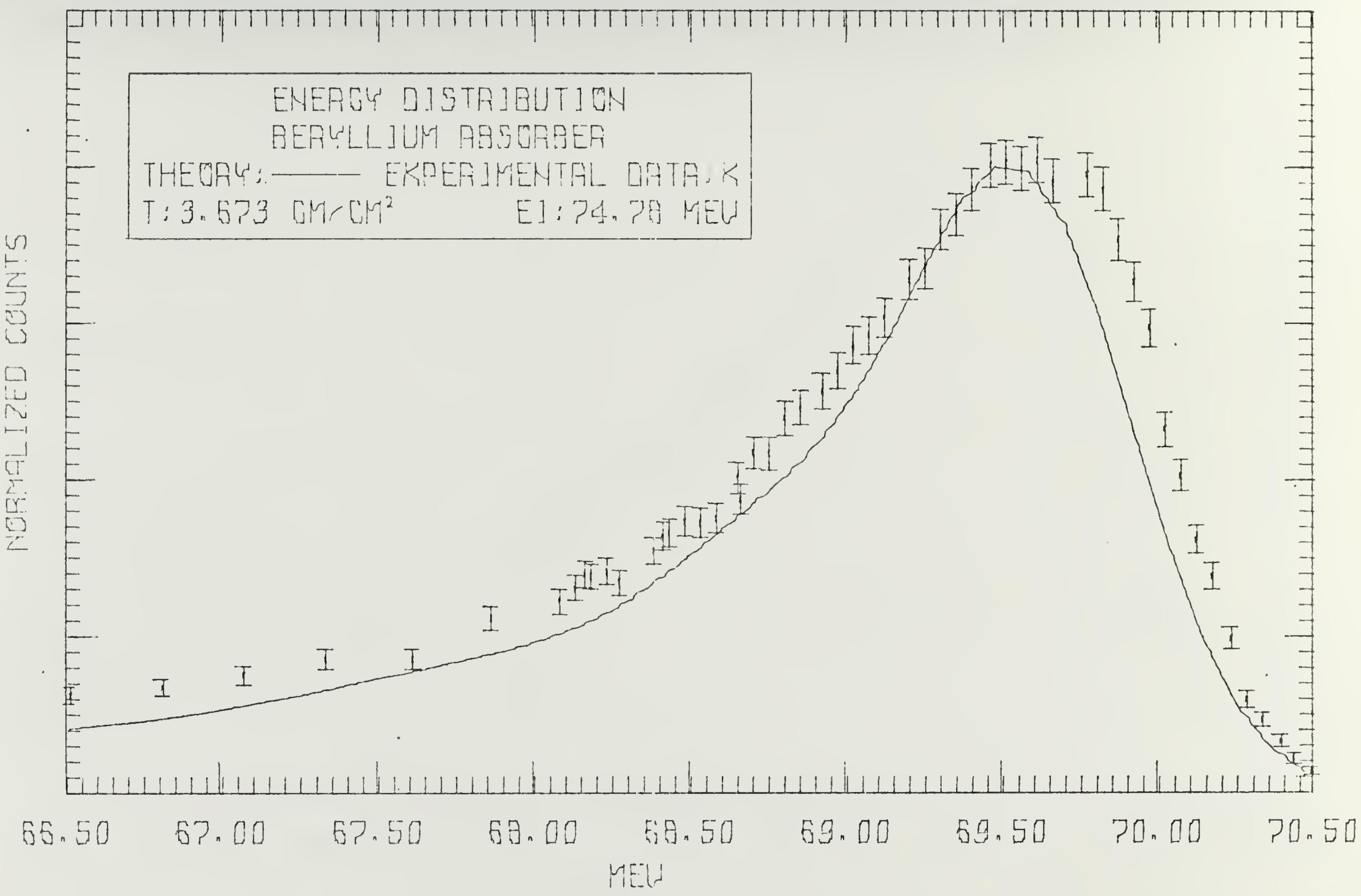
ENERGY DISTRIBUTION
BERYLLIUM ABSORBER
THEORY: ——— EXPERIMENTAL DATA: I
T: 3.673 GM/CM²
EI: 74.78 MEV
NORMALIZED COUNTS
66.50
67.00
67.50
68.00
68.50
69.00
69.50
70.00
70.50
MEV

Figure 18

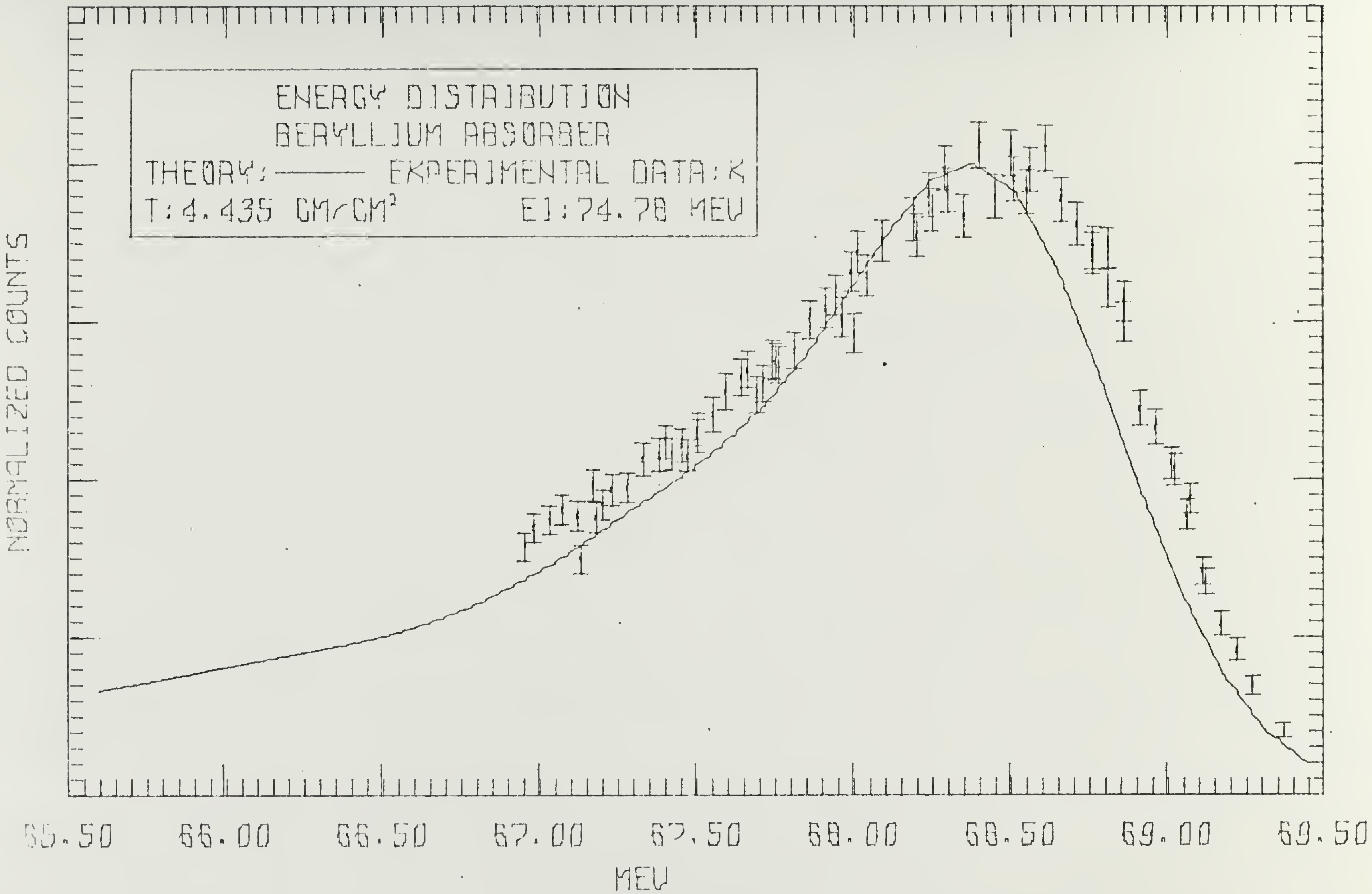
ENERGY DISTRIBUTION
BERYLLIUM ABSORBER
THEORY: ——— EXPERIMENTAL DATA: I
T: 4.435 GM/CM² E1: 74.78 MEV
NORMALIZED COUNTS
65.50
66.00
66.50
67.00
67.50
68.00
68.50
69.00
69.50
MEV

Figure 19

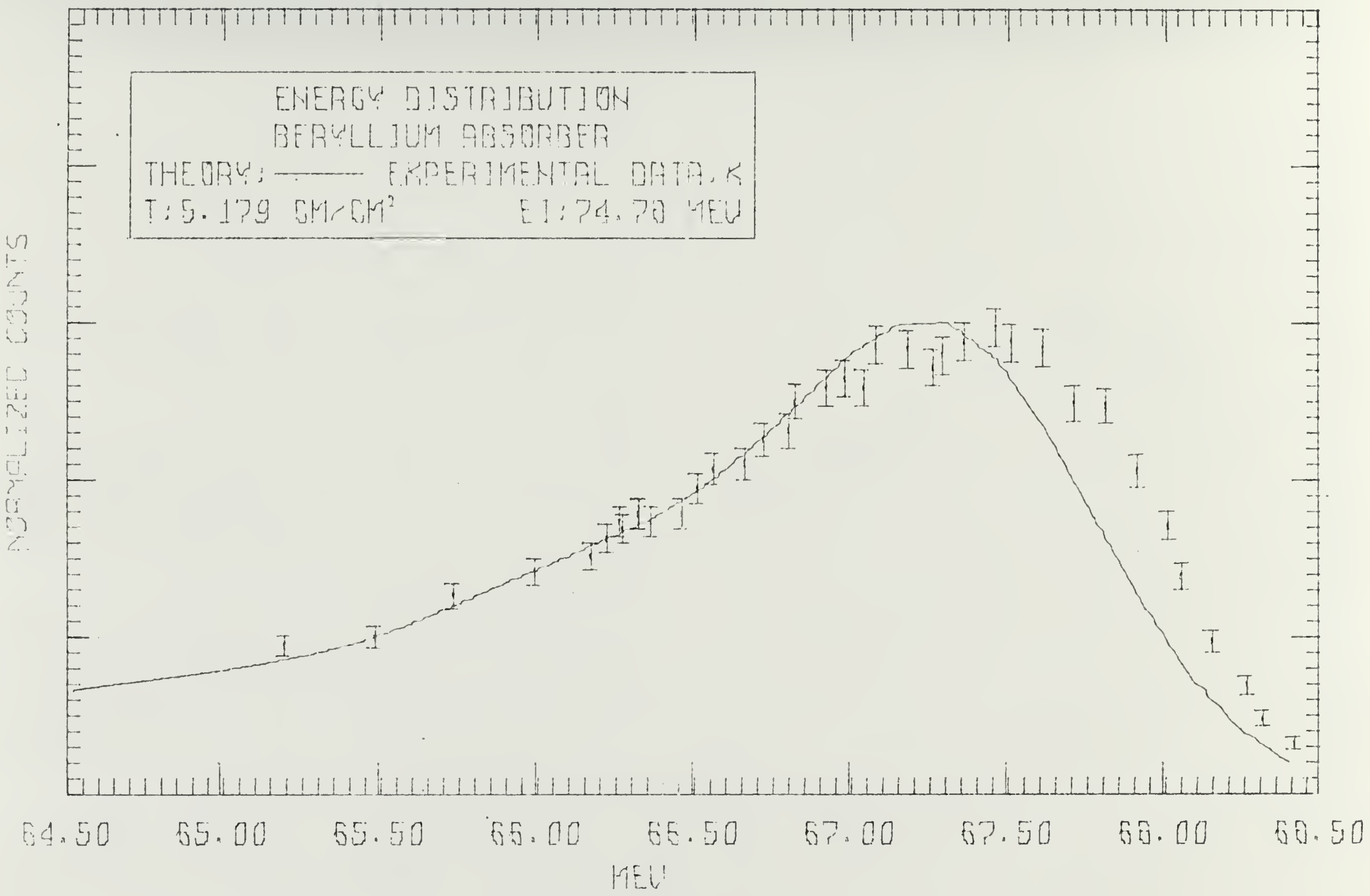
ENERGY DISTRIBUTION
BERYLLIUM ABSORBER
THEORY: ——— EXPERIMENTAL DATA, K
T: 5.179 GM/CM²
EI: 74.70 MEV
NORMALIZED COUNTS
64.50
65.00
65.50
66.00
66.50
67.00
67.50
68.00
68.50
MEV

Figure 20

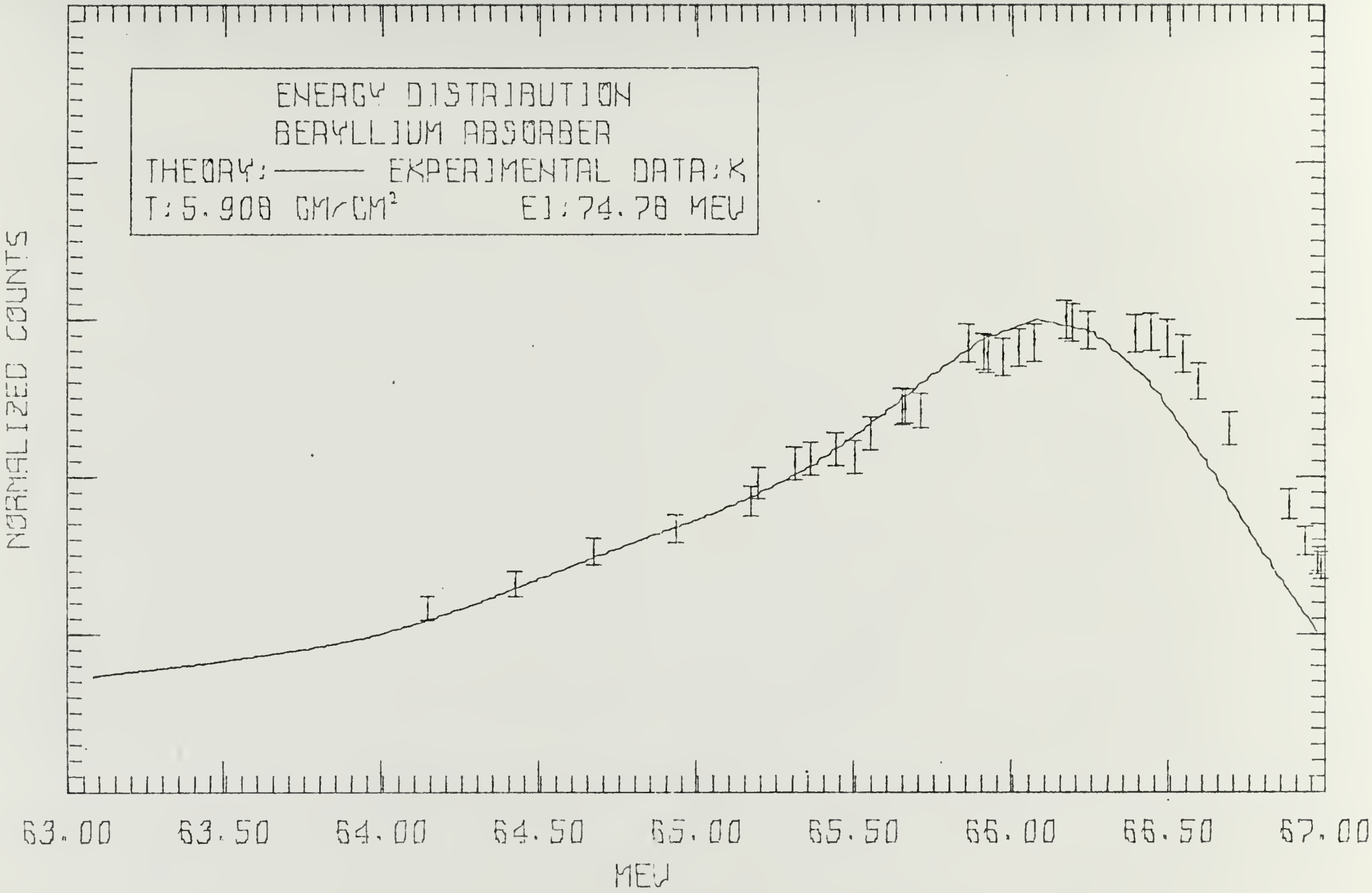
ENERGY DISTRIBUTION
BERYLLIUM ABSORBER
THEORY:——— EXPERIMENTAL DATA:K
T:5.908 GM/CM²
EI:74.78 MEV
NORMALIZED COUNTS
63.00
63.50
64.00
64.50
65.00
65.50
66.00
66.50
67.00
MEV

Figure 21

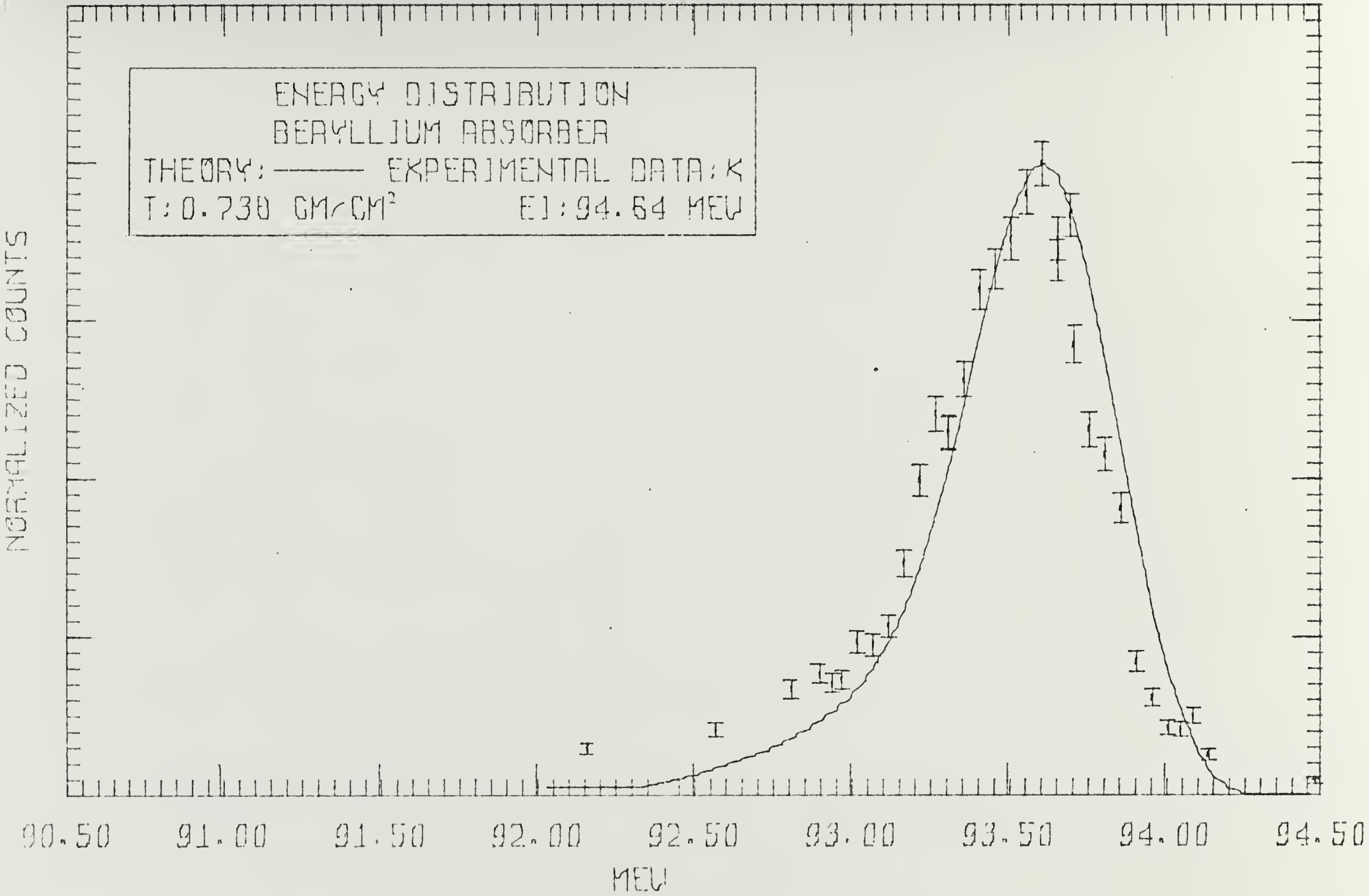
ENERGY DISTRIBUTION
BERYLLIUM ABSORBER
THEORY: ——— EXPERIMENTAL DATA: K
T: 0.730 GM/CM²
EI: 94.64 MEV
NORMALIZED COUNTS
90.50
91.00
91.50
92.00
92.50
93.00
93.50
94.00
94.50
MEV

Figure 22

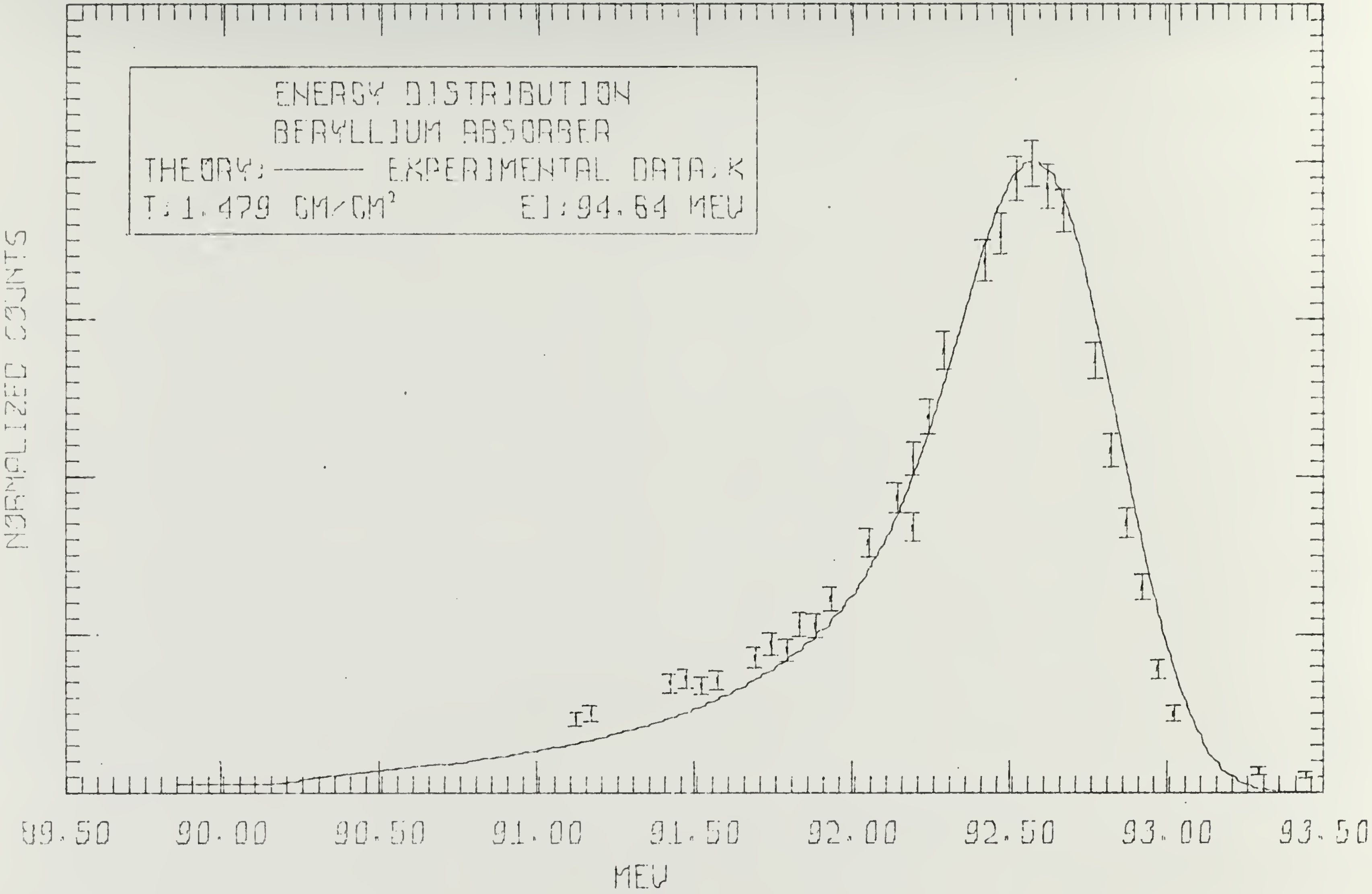
ENERGY DISTRIBUTION
BERYLLIUM ABSORBER
THEORY: ——— EXPERIMENTAL DATA; K
T: 1.479 GM/CM²
EI: 94.64 MEV
NORMALIZED COUNTS
89.50
90.00
90.50
91.00
91.50
92.00
92.50
93.00
93.50
MEV

Figure 23

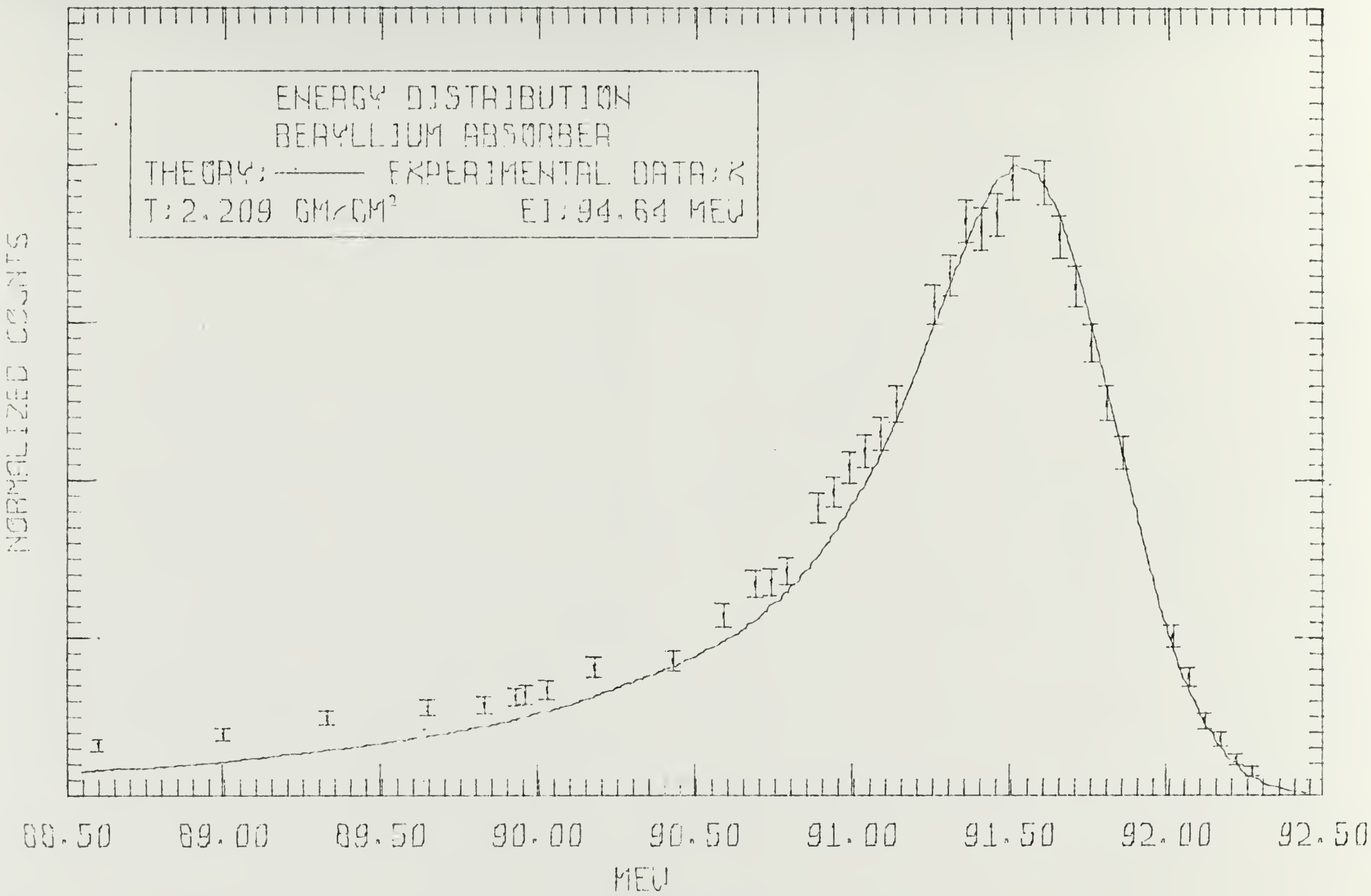
ENERGY DISTRIBUTION
BERYLLIUM ABSORBER
THEORY: ——— EXPERIMENTAL DATA: ⌶
T: 2.209 GM/CM²
EI: 94.64 MEV
NORMALIZED COUNTS
88.50
89.00
89.50
90.00
90.50
91.00
91.50
92.00
92.50
MEV

Figure 24

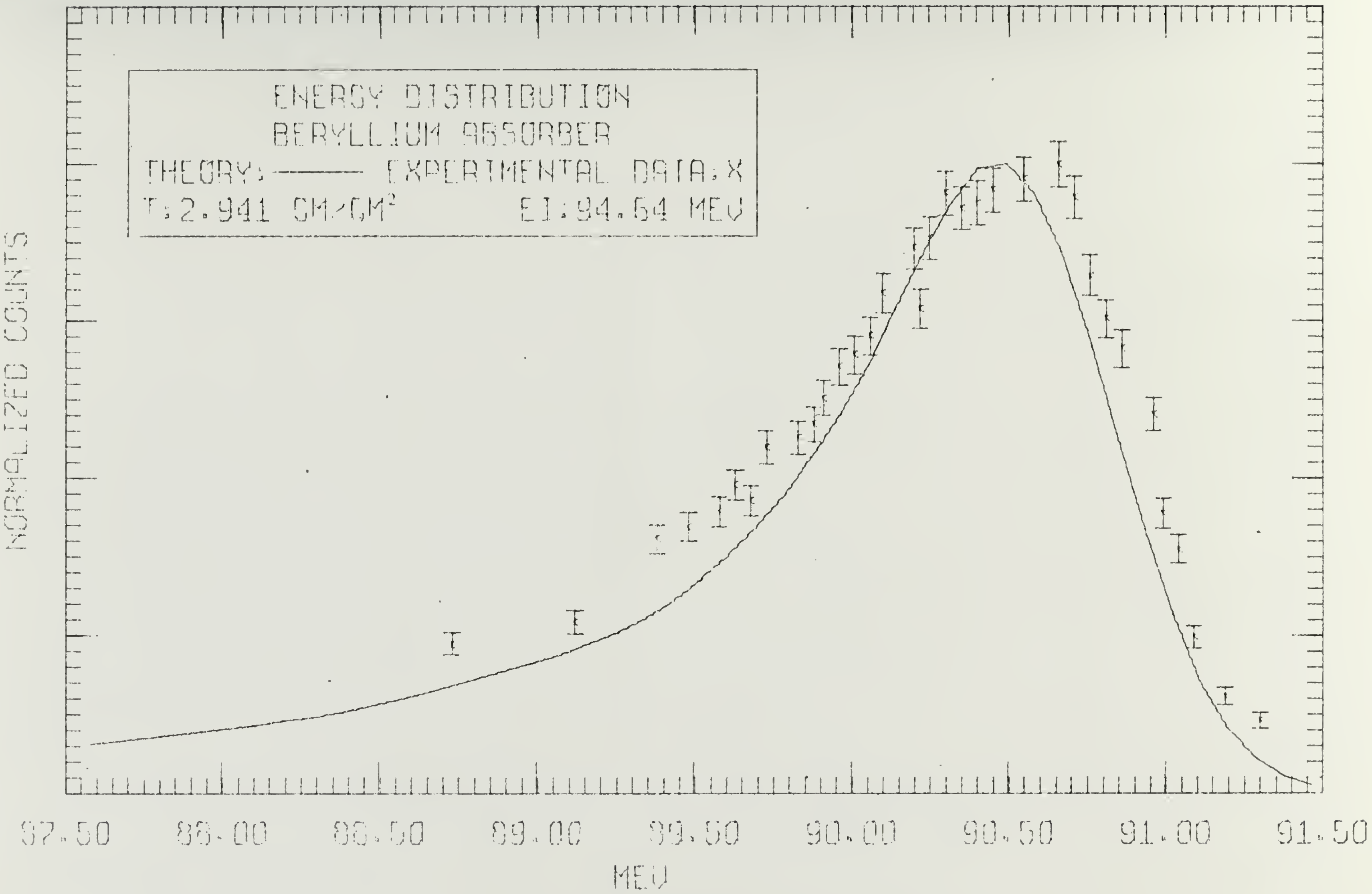
ENERGY DISTRIBUTION
BERYLLIUM ABSORBER
THEORY: ——— EXPERIMENTAL DATA: X
T: 2.941 GM/CM²
EI: 94.64 MEV
NORMALIZED COUNTS
87.50
88.00
88.50
89.00
89.50
90.00
90.50
91.00
91.50
MEV

Figure 25

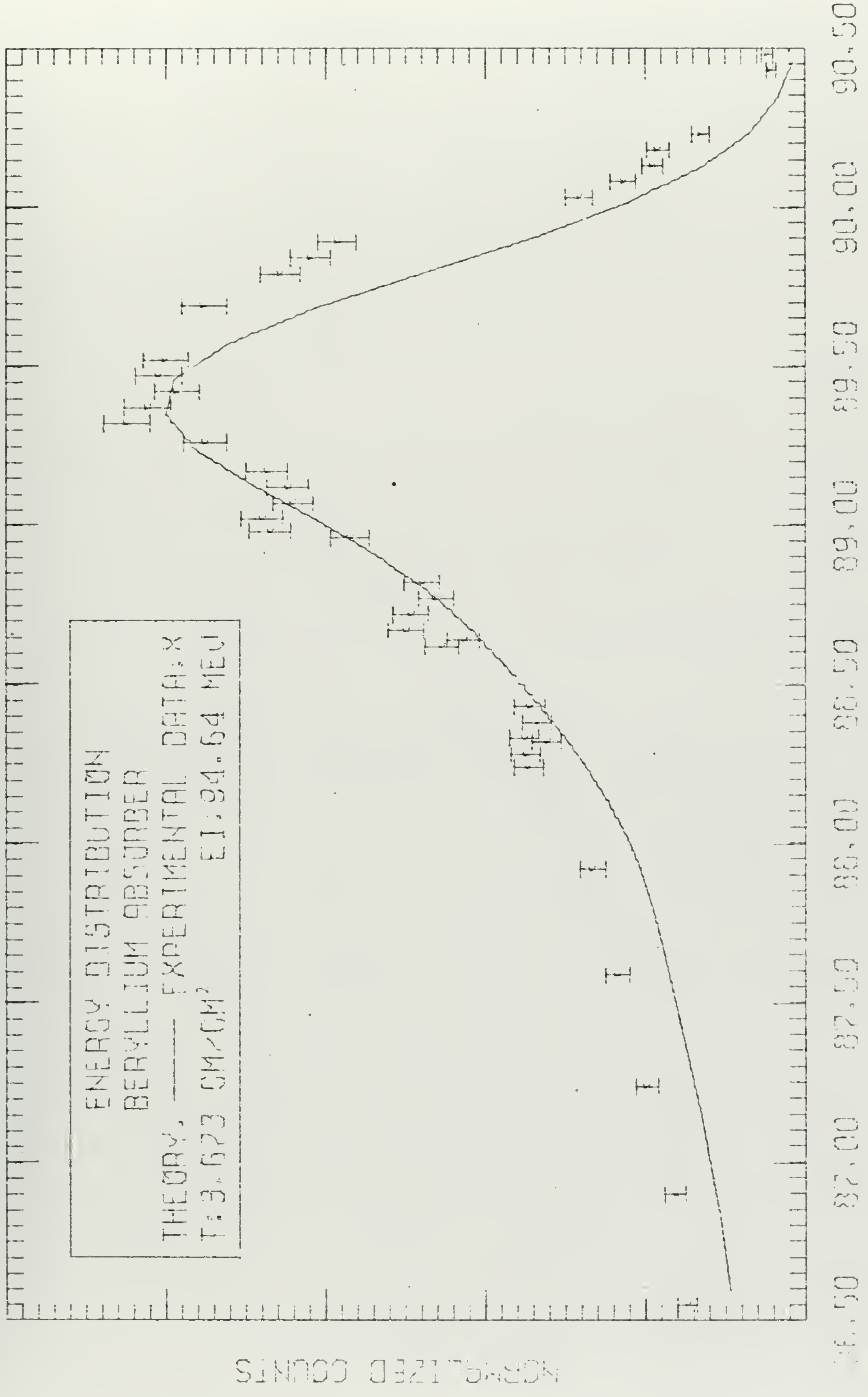
ENERGY DISTRIBUTION
BERYLLIUM ABSORBER
THEORY, —— EXPERIMENTAL DATA: X
T: 3.623 GM/CM²
EI: 94.64 MEV
86.50
87.00
87.50
88.00
88.50
89.00
89.50
90.00
90.50
MEV
NORMALIZED COUNTS

Figure 26

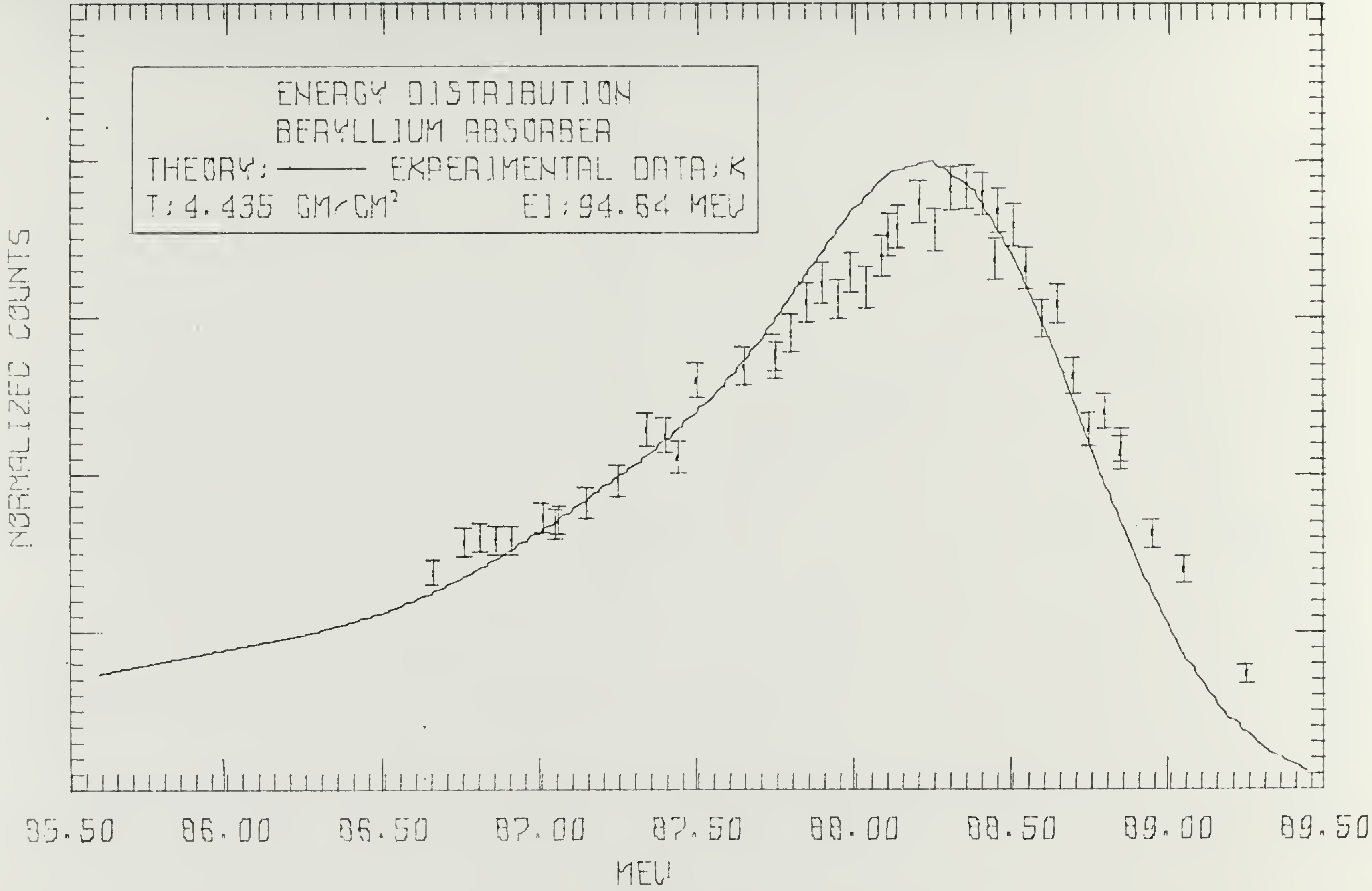
ENERGY DISTRIBUTION
BERYLLIUM ABSORBER
THEORY; ——— EXPERIMENTAL DATA; K
T; 4.435 GM/CM²
EI; 94.64 MEV
NORMALIZED COUNTS
85.50
86.00
86.50
87.00
87.50
88.00
88.50
89.00
89.50
MEV

Figure 27

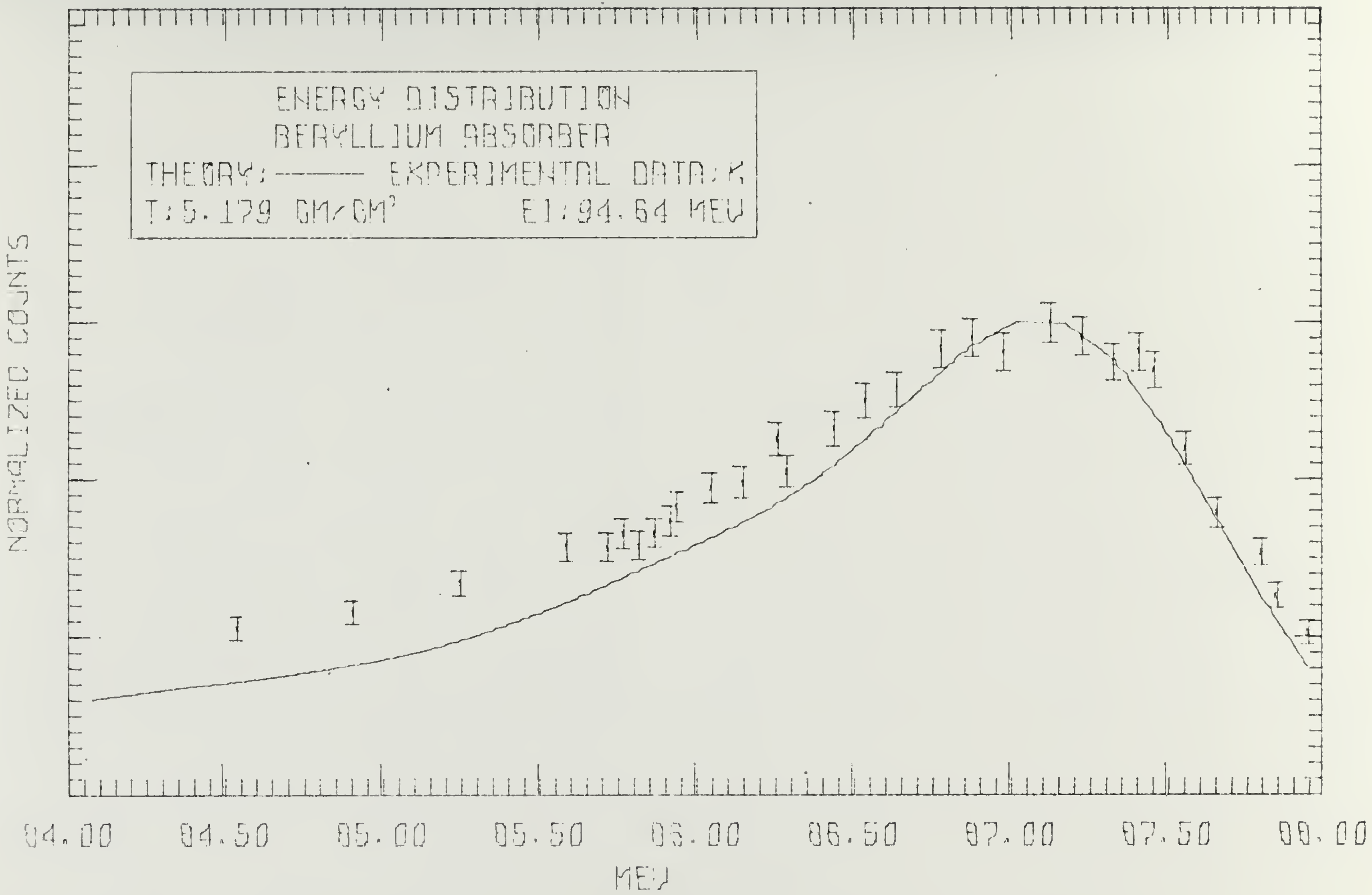
ENERGY DISTRIBUTION
BERYLLIUM ABSORBER
THEORY: ——— EXPERIMENTAL DATA: I
T: 5.179 GM/CM²
E1: 94.64 MEV
NORMALIZED COUNTS
84.00
84.50
85.00
85.50
86.00
86.50
87.00
87.50
88.00
MEV

Figure 28

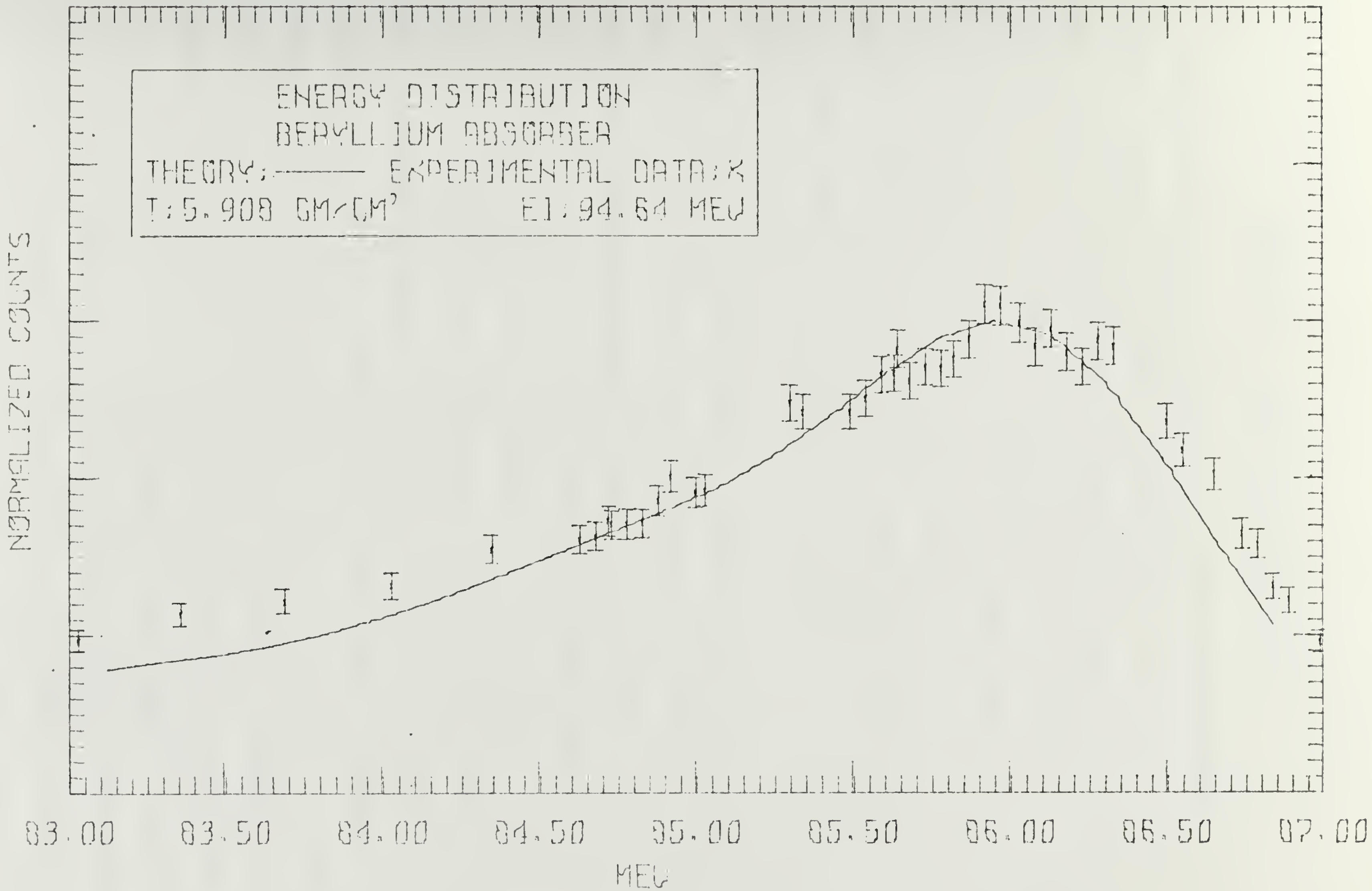
ENERGY DISTRIBUTION
BERYLLIUM ABSORBER
THEORY:——— EXPERIMENTAL DATA:X
T:5.908 GM/CM²
E1:94.64 MEV
NORMALIZED COUNTS
83.00
83.50
84.00
84.50
95.00
85.50
86.00
86.50
87.00
MEV

Figure 29

APPENDIX C - BEAM FOLDING TECHNIQUE

The theory of Blunck and Westphal [3] assumes that the beam of electrons striking the absorber is monoenergetic. The beam of electrons produced by the Naval Postgraduate School LINAC, or any other linear accelerator, for that matter, has a finite energy spread about a maximum or most probable energy point. The fact that monoenergetic electrons are not available to strike the absorber must be taken into account in computing theoretical predictions if a meaningful comparison with experimental results is to be made. This has been done here by a technique termed "beam folding".

Beam folding is accomplished by a number of well defined steps. Energy distribution curves may be approximated by histograms. These histograms consist of a series of "bins" of area $W(Q)\Delta Q$, where Q is the energy loss and $W(Q)\Delta Q$ is the probability of loss between Q and $Q + \Delta Q$. Thus, each bin has an "address", Q, on an energy coordinate scale. To accomplish beam folding, the beam distribution must be known. This is observed experimentally and approximated in the computer by a gaussian curve of appropriate half-width. The energy at which the maximum occurs is established by the energy of the beam and the magnitude of energy loss incurred by elastic scattering of the beam as it impinges on the thin aluminum scattering foil prior to striking the absorber. The width ΔQ is then selected for the predicted distribution. This must be a small, but finite number where numerical techniques are to be used. This same width is used to break the beam distribution into a histogram. This is illustrated in Figure 30(a). The reason the same width is used for both distributions is to facilitate computer programming.

(a) Beam Distribution

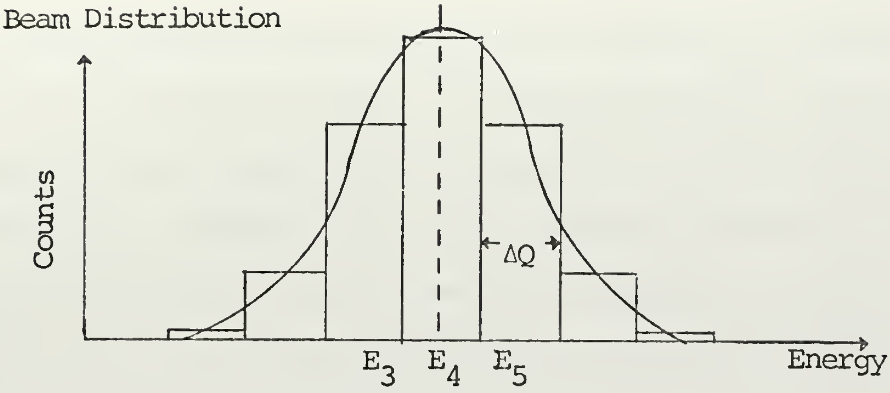

(b) Energy Distribution of E_4

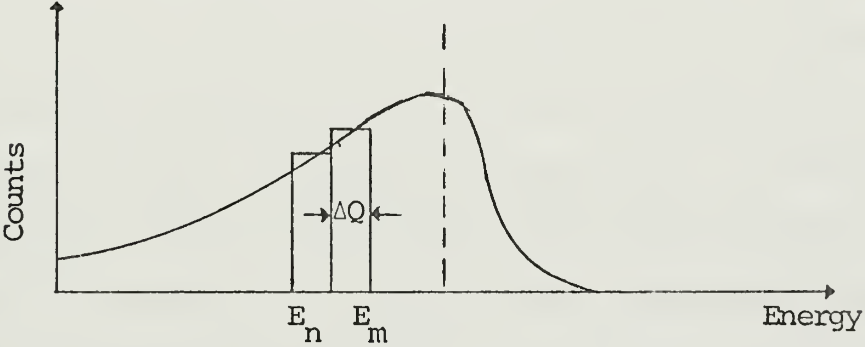

(c) Energy Distribution of E_5

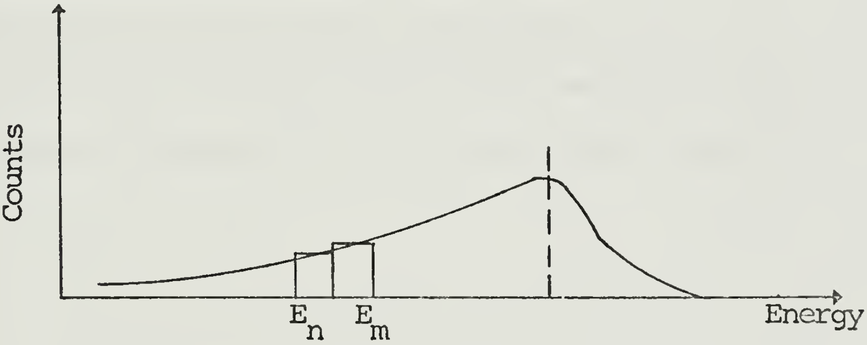

(d) Total Energy Distribution

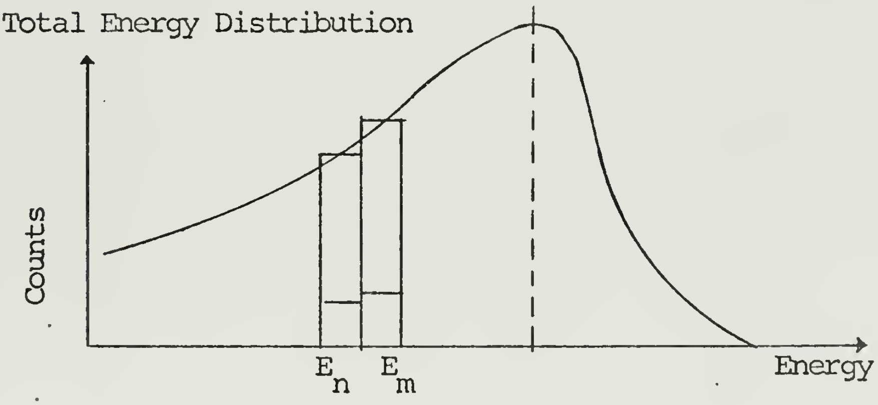

Figure 30. Beam Folding Distributions

Each bin of the beam distribution is now treated as a monoenergetic beam with energy commensurate with its center location on the energy scale. Each bin also has a definite magnitude, or weight, with the magnitude of the center bin being unity. The formulae of Blunck and Westphal is now applied to each of these beams and an absorber distribution curve results for each, with a maximum amplitude proportional to the height of the appropriate beam distribution histogram. Each of the absorber distribution curves thus obtained may be thought of as being plotted and added to previously determined curves, using the energy of the electrons as a correlation point, as depicted in Figures 30(b), (c) and (d). This is accomplished on the computer by adding the contents of each bin of the same address and plotting the cumulative total. The bin of address E_x is depicted in Figures 30(b), (c) and (d). Note that the beam distribution for histogram E4 is centered over the maximum point of the distribution. This is important as a false picture could easily be presented if the histogram were not symmetrical as the distribution would then appear skewed.

APPENDIX D - COMPUTER PROGRAM

```
C PURPOSE: THIS PROGRAM ACCEPTS PARAMETERS FROM ENERGY LOSS
C    EXPERIMENTS CONDUCTED ON THE LINAC AND WILL COMPUTE
C    THEORETICAL HALFWIDTH AND MOST PROBABLE ENERGY LOSS AND
C    WILL PLOT BOTH THE EXPERIMENTAL AND THEORETICAL ENERGY
C    DISTRIBUTION FOR THE EXPERIMENT.
C
C SCOPE: THE PROGRAM IS SET UP TO MAKE COMPUTATIONS RELATIVE
C    TO EXPERIMENTATION WITH ALUMINUM,COPPER,TIN,GADOLINIUM
C    LEAD AND BERYLLIUM.
C
C METHOD: THE PROGRAM PLOTS A THEORY CURVE BASED ON THE FIT
C    OF GAUSSIAN CURVES PERFORMED BY BLUNCK AND WESTPHAL FOR
C    THE PREDICTED ENERGY DISTRIBUTION CURVES.  THE INTEGRA-
C    TION OVER ENERGY LOSS INDICATED IN THE AFOREMENTIONED
C    PAPER IS PERFORMED ON THE COMPUTER USING 32 POINT GAUSS
C    QUADRATURE.  TWO GRAPHS ARE PLOTTED; ONE REPRESENTS THE
C    B-W PREDICTION WITH A MONENERGETIC BEAM OF ELECTRONS AND
C    THE OTHER, WHICH ALSO HAS EXPERIMENTAL RESULTS THEREON,
C    REPRESENTS THE SAME THEORY WITH A POLYENERGETIC BEAM
C    DISTRIBUTION FOLDED IN.
C
C THIS PROGRAM IS WRITTEN USING FORTRAN IV LANGUAGE AND THE
C    NPS COMPUTER FACILITY PLOTTING PACKAGE.  TOTAL RUNNING
C    TIME IS A FUNCTION OF THICKNESS, ATOMIC NUMBER, AND
C    HALFWIDTH.
C
      IMPLICIT REAL*8(A-H,O-Z)
C
C ESTABLISH TITLES FOR PLOTS.
C
      REAL*8 T1(4)
      DATA T1/'        ENERGY DISTRIBUTION        '/
      REAL*8 T3(4)
      DATA T3/'         ALUMINUM ABSORBER         '/
      REAL*8 T4(4)
      DATA T4/'T:       GM/CM        EI:       MEV'/
      REAL*8 T5(4)
      DATA T5/'         UNFOLDED  THEORY          '/
      REAL*8 T6(4)
      DATA T6/'THEORY:         EXPERIMENTAL DATA:X'/
      REAL*8 T7(4)
      DATA T7/'           LEAD ABSORBER           '/
      REAL*8 T8(4)
      DATA T8/'          TIN ABSORBER             '/
      REAL*8 T9(4)
      DATA T9/'        GADOLINIUM ABSORBER        '/
      REAL*8 T10(4)
      DATA T10/'       COPPER ABSORBER             '/
      REAL*8 T11(4)
      DATA T11/'        BERYLLIUM ABSORBER         '/
      DIMENSION E(50),WF(50),WQT(300),HW(300),XX(300),
     1WUF(300),XUF(300),EXX(200),EXY(200),IXY(200),T2(4)
      EXTERNAL FCT,BEAM,WION,WRAD
      DO1200 J=1,5
      E(J)=0
 1200 WF(J)=0
      DO1201 J=1,200
      EXX(J)=0
      EXY(J)=0
 1201 IXY(J)=0
      DO1202 J=1,300
      WQT(J)=0
      HW(J)=0
      XX(J)=0
      WUF(J)=0
 1202 XUF(J)=0
```

```
C READ IN PARAMETERS FOR EXPERIMENT.
C    EB        BEAM ENERGY
C    Z         ATOMIC NUMBER
C    A         ATOMIC WEIGHT
C    T         TARGET THICKNESS: GM/SQ CM
C    QZERO     SPECTROMETER INDICATION OF LOCATION OF BEAM
C                 DISTRIBUTION (MEV)
C    CTSNOR    NUMBER TO WHICH EXPERIMENTAL COUNTS WILL BE
C                 NORMALIZED
C    HT        HALFWIDTH OF BEAM DISTRIBUTION
      READ(5,11) EB,Z,A,T,QZERO,CTSNOR,HT
      WRITE(6,21) EB,Z,A,T,QZERO,CTSNOR,HT
   21 FORMAT(/,2X,' EB: ',F7.2,' Z: ',F4.0,' A: ',F8.3,
     1' T: ',F7.4,' QZERO: ',F5.3,' CTSNOR: ',F6.1,
     2' HT: ',F5.3,/)
C
C DIVIDE ZERO PEAK INTO "BINS" OF WIDTH DELX.  BIN WIDTH
C    INCREASES WITH TARGET THICKNESS.
C
      DELX=.03*T
      IF(T.LT.1.) DELX=.06*T
C
C QAVE IS THE RECOIL LOSS OF ELECTRONS STRIKING ALUMINUM
C    NUCLEII OF THE SCATTERING FOIL.  IONIZATION LOSS IN
C    SCATTERER IS NEGLECTED.
C
      QAVE=EB*EB/(931.4*27.)
C
C CORR IS THE CORRECTION TO BE ADDED TO EXPERIMENTAL ENERGY
C    TO CORRECT FOR SPECTROMETER ERROR.
C
      CORR=QZERO-QAVE
   12 FORMAT(5(1X,F8.3,1X,I6))
C
C READ IN UP TO 200 EXPERIMENTAL POINTS; EXX IS ENERGY (MEV)
C    AND IXY IS COUNTS.  THERE MUST BE 40 DATA CARDS AND THE
C    LAST EXX MUST BE ZERO.
C
      READ(5,12) (EXX(J),IXY(J),J=1,200)
C
C ESTABLISH PARAMETERS FOR SCATTERING FOIL.
C
      FOIL=.00686
      ZFOIL=13.
      KSIG=0
      DO 1 J=1,200
    1 EXY(J)=IXY(J)
      M=0
C
C EI IS VALUE OF BEAM ENERGY INCIDENT ON TARGET.
C
      EI=EB-QAVE
      TEMP=EI
C
C THE FOLLOWING PORTION OF THE PROGRAM UNFOLDS BEAM DISTRI-
C    BUTION.  ICENT IS AN INTEGER VALUE ASSIGNED TO THE
C    HISTOGRAM CENTERED OVER THE PEAK OF THE BEAM DISTRIBU-
C    TION.  EACH HISTOGRAM IS DENOTED BY ITS ENERGY E AND
C    MAGNITUDE RELATIVE TO THE PEAK OF THE DISTRIBUTION, WF.
C
      ICENT=(HT+DELX)/DELX
      X=EI-ICENT*DELX
  202 X=X+DELX
      IF(X.GT.(EI+HT)) GOTO 1003
      M=M+1
      E(M)=X
      WF(M)=BEAM(EI,HT,X)
      GOTO202
 1003 WRITE(6,22) QAVE,HT,FOIL,ZFOIL,EI
      DO 1006 L=1,M
      DX=0
      N=0
```

```
 1005 N=N+1
C
C USING EACH HISTOGRAM AS A "BEAM", THE FOLLOWING PORTION OF
C    THE PROGRAM COMPUTES AN ENERGY DISTRIBUTION FOR EACH
C    OF THESE "BEAMS" AND STORES THEM IN "BINS" LABELED BY
C    ENERGY, XX.  THE CUMULATIVE AMOUNT OF ELECTRON COUNTS IN
C    THE BIN IS WQT.  Q IS THE ENERGY LOSS OVER WHICH THE B-W
C    PREDICTION IS INTEGRATED AND DX IS THE AMOUNT BY WHICH
C    Q CHANGES FOR EACH SUCCESSIVE INTEGRATION.  INTEGRATION
C    IS CARRIED OUT IN SUBROUTINE DQG32.
C
      DX=DX+DELX
      IF(Z.LT.10.) GO TO 333
      Q=3.0*T*(Z/13.)**.50-DX
      GO TO 334
  333 Q=3.0*T*(Z/4.)**.50-DX
  334 IF(Q.LT.EI) GO TO 1004
      N=0
      GOTO1005
 1004 IF(Q.LT.0)GOTO1006
      EI=E(L)
      XL=.00000001*Q
      VALIM=.25*Q
      CALL DQG32(0.,XL    ,FCT,ZA,EI,Q,T,A,Z)
      CALL DQG32(XL,VALIM,FCT,ZB,EI,Q,T,A,Z)
      CALL DQG32(VALIM,Q ,FCT,ZC,EI,Q,T,A,Z)
      WQ=ZA+ZB+ZC
      WQT(L+N-1)=WQT(L+N-1)+WQ*WF(L)
      XX(L+N-1)=E(L)-Q
      J=L+N-1
C
C THE DISTRIBUTION FOR THE HISTOGRAM CORRESPONDING TO THE
C    CENTER OF THE BEAM DISTRIBUTION IS REMOVED AND STORED IN
C    WUF AND XUF AS THE UNFOLDED COUNTS AND ENERGY
C    RESPECTIVELY.
C
      IF(L.NE.ICENT)GOTO1005
      WUF(N)=WQ
      XUF(N)=EI-Q
      K=N
      GOTO 1005
 1006 CONTINUE
      DO 1717 I=1,7
C
C ELIMINATE LOW NUMBERED "BINS" AS THEY ARE ONLY PARTLY FIL-
C    LED AND ARE NOT REPRESENTATIVE OF THE CUMULATIVE
C    DISTRIBUTION.
C
      WUF(I)=WUF(8)
 1717 WQT(I)=WQT(8)
      DO 6 I=1,4
    6 T3(I)=T6(I)
      GOTO 779
  777 DO778 N=1,K
C
C PROCESS THE UNFOLDED THEORY CURVE.  SETTING EXX(1) EQUAL
C    TO ZERO ALLOWS PLOTTING OF THIS THEORY CURVE WITHOUT ANY
C    EXPERIMENTAL DATA.
C
      WQT(N)=WUF(N)
      XX(N)=XUF(N)
      KSIG=1
      J=K
  778 CONTINUE
      EXX(1)=0
      DO 5 I=1,4
    5 T3(I)=T5(I)
  779 WQTMX=0
      DO1007 N=3,J
C
C DETERMINE THE MAXIMUM POINT OF THE DISTRIBUTION, WQTMX,
C    AND THUS ESTABLISH THE MOST PROBABLE ENERGY LOSS, QP.
```

```
      IF(WQT(N).LE.WQT(N-1).AND.WQT(N-1).GE.WQT(N-2))
     1GOTO1008
      GOTO 1007
 1008 IF(WQT(N-1).LT.WQTMX)GOTO 1007
      WQTMX=WQT(N-1)
      EI=TEMP
      QP=EI-XX(N-1)
 1007 CONTINUE
C
C NORMALIZE ALL POINTS OF DISTRIBUTION AND STORE IN HW.
C
      DO 1009 M=1,J
      HW(M)=WQT(M)/WQTMX
 1009 CONTINUE
      J=J-1
      HWI=0
C
C DETERMINE HALFWIDTH OF THE THEORETICAL DISTRIBUTION, HWA.
C
      DO 1010 M=1,J
      IF(HW(M+1).GT..5.AND.HW(M).LT..5)HWI=XX(M)+(.5-
     1HW(M))*DELX/(HW(M+1)-HW(M))
      IF(M.EQ.J.AND.HWI.EQ.0)GOTO119
      GOTO121
  119 WRITE(6,20)
      HWA=0
      GOTO1010
   20 FORMAT(/,2X,'NO HALFWIDTH OBTAINED')
  121 IF(HW(M).GT..5.AND.HW(M+1).LT..5)HWA=XX(M)+(HW(M)
     1-.5)*DELX/(HW(M)-HW(M+1))-HWI
 1010 CONTINUE
C
C ESTABLISH CUTOFF SIGNAL FOR PLOTTING SUBROUTINE AND
C    ESTABLISH CORRECT GRAPH TITLES FOR ABSORBER USED.
C
      XX(J+1)=0
      IF(Z.GT.4.1)GOTO13
      DO 2 I=1,4
    2 T2(I)=T11(I)
      GOTO1011
   13 IF(Z.GT.13.1)GOTO29
      DO 3 I=1,4
    3 T2(I)=T3(I)
      GOTO1011
   29 IF(Z.GT.29.1)GOTO50
      DO 10I=1,4
   10 T2(I)=T10(I)
      GOTO1011
   50 IF(Z.GT.50.1)GOTO64
      DO 8 I=1,4
    8 T2(I)=T8 (I)
      GOTO1011
   64 IF(Z.GT.64.1)GOTO82
      DO 9 I=1,4
    9 T2(I)=T9 (I)
      GOTO1011
   82 DO 7 I=1,4
    7 T2(I)=T7 (I)
C
C SEND DATA TO PLOTTING SUBROUTINE FOR PROCESSING AND
C    PRINT RESULTS OF COMPUTATIONS IN TABULAR FORM.
C
 1011 CALL GRAPH(XX,WQT,EXX,EXY,T4,T3,T2,T1,HWA,EI,T,
     1CORR,CTSNOR,QP)
      WRITE(6,22) QP,HWA,T,Z,EI
      IF(KSIG.EQ.0) GOTO 777
   11 FORMAT(7F10.0)
   22 FORMAT(/,2X,' QP: ',F7.4,' HALF WIDTH: ',F6.3,
     1' T(GM/SQ-CM): ',F6.4,' Z: ',F4.0,' INCIDENT ENERGY: '
     2,F5.2,/)
      STOP
      END
```

```
      SUBROUTINE DQG32(XL,XU,FCT,Y,EI,Q,T,D,Z)
C
C PURPOSE: THIS SUBROUTINE PERFORMS THE INTEGRATION REQUIRED
C    IN THE B-W THEORY.
C
      IMPLICIT REAL*8(A-H,O-Z)
      A=.5D0*(XU+XL)
      B=XU-XL
      C=.49863193092474078D0*B
      Y=.35093050047350483D-2*
     1(FCT((A+C),Z,D,T,EI,Q)+FCT((A-C),Z,D,T,EI,Q))
      C=.49280575577263417D0*B
      Y=Y+.8137197365452835D-2*
     1(FCT((A+C),Z,D,T,EI,Q)+FCT((A-C),Z,D,T,EI,Q))
      C=.48238112779375322D0*B
      Y=Y+.12696032654631030D-1*
     1(FCT((A+C),Z,D,T,EI,Q)+FCT((A-C),Z,D,T,EI,Q))
      C=.46745303796886984D0*B
      Y=Y+.17136931456510717D-1*
     1(FCT((A+C),Z,D,T,EI,Q)+FCT((A-C),Z,D,T,EI,Q))
      C=.44816057788302606D0*B
      Y=Y+.21417949011113340D-1*
     1(FCT((A+C),Z,D,T,EI,Q)+FCT((A-C),Z,D,T,EI,Q))
      C=.42468380686628499D0*B
      Y=Y+.25499029631188088D-1*
     1(FCT((A+C),Z,D,T,EI,Q)+FCT((A-C),Z,D,T,EI,Q))
      C=.39724189798397120D0*B
      Y=Y+.29342046739267774D-1*
     1(FCT((A+C),Z,D,T,EI,Q)+FCT((A-C),Z,D,T,EI,Q))
      C=.36609105937014484D0*B
      Y=Y+.32911111388180923D-1*
     1(FCT((A+C),Z,D,T,EI,Q)+FCT((A-C),Z,D,T,EI,Q))
      C=.33152213346510760D0*B
      Y=Y+.36172897054424253D-1*
     1(FCT((A+C),Z,D,T,EI,Q)+FCT((A-C),Z,D,T,EI,Q))
      C=.29385787862038116D0*B
      Y=Y+.39096947893535153D-1*
     1(FCT((A+C),Z,D,T,EI,Q)+FCT((A-C),Z,D,T,EI,Q))
      C=.25344995446611470D0*B
      Y=Y+.41655962113473378D-1*
     1(FCT((A+C),Z,D,T,EI,Q)+FCT((A-C),Z,D,T,EI,Q))
      C=.21067563806531767D0*B
      Y=Y+.43826046502201906D-1*
     1(FCT((A+C),Z,D,T,EI,Q)+FCT((A-C),Z,D,T,EI,Q))
      C=.16593430114106382D0*B
      Y=Y+.45586939347881942D-1*
     1(FCT((A+C),Z,D,T,EI,Q)+FCT((A-C),Z,D,T,EI,Q))
      C=.11964368112606854D0*B
      Y=Y+.46922199540402283D-1*
     1(FCT((A+C),Z,D,T,EI,Q)+FCT((A-C),Z,D,T,EI,Q))
      C=.7223598079139825D-1*B
      Y=Y+.47819360039637430D-1*
     1(FCT((A+C),Z,D,T,EI,Q)+FCT((A-C),Z,D,T,EI,Q))
      C=.24153832843869158D-1*B
      Y=B*(Y+.48270044257363900D-1*
     1(FCT((A+C),Z,D,T,EI,Q)+FCT((A-C),Z,D,T,EI,Q)))
      RETURN
      END
```

```
      REAL FUNCTION WION*8(X,EI,T,Z,A,Q )
C
C PURPOSE: THIS FUNCTION CALCULATES THAT PART OF THE ENERGY
C   DISTRIBUTION OF AN ELECTRON DUE TO LOSS OF ENERGY BY
C   IONIZATION WHILE PASSING THROUGH AN ABSORBER.
C
      IMPLICIT REAL*8(A-H,O-Z)
C
C IL ARE THE AVERAGE IONIZATION POTENTIALS PER ELECTRON FOR
C.  LEAD FOR EACH SHELL, BEGINNING WITH THE K SHELL.
C
C NPOTL IS THE NUMBER OF IONIZATION POTENTIALS USED FOR LEAD
C
C IN THIS CONTEXT, L=LEAD, G=GADULINIUM, S=TIN, C=COPPER,
C   A=ALUMINUM, AND B=BERYLLIUM.
C
      REAL*8 IL(6)/.088000,.014700,.003200,.000490,
     1.000076,.000002/
      REAL*8 NL(6)/2.,8.,18.,32.,18.,4./
      REAL*8 IG(5)/.05024,.00785,.00189,.00024,.000026/
      REAL*8 NG(5)/2.,8.,18.,25.,9./
      REAL*8 IS(5)/.0292,.0044,.00072,.000062,.000001/
      REAL*8 NS(5)/2.,8.,18.,18.,4./
      REAL*8 IC(3)/.00898,.00099,.000068/
      REAL*8 NC(3)/2.,8.,18./
      REAL*8 IA(2)/.00156,.000088/
      REAL*8 NA(2)/2.,8./
      REAL*8 IB(2)/.000148,.000014/
      REAL*8 NB(2)/2.,2./
      NPOTL=6
      NPOTG=5
      NPOTS=5
      NPOTC=3
      NPOTA=2
      NPOTB=2
C
C SB IS THE SUMMATION OF IONIZATION POTENTIALS FOR THE
C   EXPERIMENTAL ATOM.
C
      SB=0.
C
C XMASE IS THE REST MASS OF AN ELECTRON IN MEV.
C
      XMASE=.511006
C
C BETA IS THE NORMAL V/C USED IN RELATIVISTIC CALCULATIONS.
C
C GAMMA IS THE NORMAL TERM USED IN RELATIVISTIC CALCULATIONS
C
      BETA=DSQRT((EI*EI+2.*EI*XMASE)/(EI*EI+2.*EI*XMASE
     1+XMASE*XMASE))
      GAMMA=1./(1.-BETA**2)**(1./2.)
C
C AT THIS POINT, THE PROGRAM MUST COMPUTE THE PROPER CON-
C   STANTS FOR THE EXPERIMENTAL Z.  A SERIES OF LOGIC STATE-
C   MENTS SELECT THE CORRECT FORMULAE.
C   SEE ALUMINUM AS EXAMPLE.
C
      IF(Z.GT.4.1)GOTO13
      DO 70 I=1,NPOTB
      B=IB(I)*NB(I)*DLOG(2.*EI/(IB(I)*(1.-BETA**2)))
   70 SB=SB+B
      B2=18.64
      A1=.0081
      DELT=4.606*DLOG10(BETA*GAMMA)-2.83
C
C DELT=4.606X+C FOR BERYLLIUM.  SEE STERNHEIMER.
      GO TO 111
   13 IF(Z.GT.13.1)GOTO29
C
C COMPUTE SB FOR EXPERIMENTAL Z.  B IS THE IONIZATION POTEN-
C   TIAL FROM ONE SHELL.
```

```
      DO 71 I=1,NPOTA
      B=IA(I)*NA(I)*DLOG(2.*EI/(IA(I)*(1.-BETA**2)))
   71 SB=SB+B
C
C ESTABLISH VALUES FOR B2 AND A1.  THESE ARE MATERIAL DE-
C   PENDENT CONSTANTS USED TO COMPUTE THE AVERAGE ENERGY
C   LOSS BY IONIZATION AND ARE SUPPLIED BY THE STERNHEIMER
C   PAPER.  THESE ARE B AND A, RESPECTIVELY, FROM HIS PAPER.
C
      B2=16.77
      A1=.0740
C
C DELT IS A PART OF THE EXPRESSION BY STERNHEIMER FOR THE
C   AVERAGE ENERGY LOSS DUE TO IONIZATION.  NUMBERS HEREIN
C   REPRESENT OTHER STERNHEIMER CONSTANTS AS FOLLOWS:
C      SMALL A   .0906
C      SMALL M   3.510
C      X1        3.000
C      -C        4.210
C
      DELT=4.606*DLOG10(BETA*GAMMA)-4.21+.0906*
     1(3.-DLOG10(BETA*GAMMA))**3.51
      GO TO 111
   29 IF(Z.GT.29.1)GOTO50
      DO 72 I=1,NPOTC
      B=IC(I)*NC(I)*DLOG(2.*EI/(IC(I)*(1.-BETA**2)))
   72 SB=SB+B
      B2=15.09
      A1=.0701
      DELT=4.606*DLOG10(BETA*GAMMA)-4.74+.1190*
     1(3.-DLOG10(BETA*GAMMA))**3.38
      GO TO 111
   50 IF(Z.GT.50.1)GOTO64
      DO 73 I=1,NPOTS
      B=IS(I)*NS(I)*DLOG(2.*EI/(IS(I)*(1.-BETA**2)))
   73 SB=SB+B
      B2=13.83
      A1=.0647
      DELT=4.606*DLOG10(BETA*GAMMA)-6.28+.404*(3.-
     1DLOG10(BETA*GAMMA))
     1**2.52
      GO TO 111
   64 IF(Z.GT.64.1)GOTO82
      DO 74 I=1,NPOTG
      B=IG(I)*NG(I)*DLOG(2.*EI/(IG(I)*(1.-BETA**2)))
   74 SB=SB+B
      B2=13.3
      A1=.0624
      DELT=4.606*DLOG10(BETA*GAMMA)-6.8+.418*(3.-
     1DLOG10(BETA*GAMMA))
     1**2.10
      GO TO 111
   82 IF(Z.GT.82.1)GOTO112
      DO 75 I=1,NPOTL
      B=IL(I)*NL(I)*DLOG(2.*EI/(IL(I)*(1.-BETA**2)))
   75 SB=SB+B
      B2=12.81
      A1=.0608
      DELT=4.606*DLOG10(BETA*GAMMA)-6.93+.0652*
     1(4.-DLOG10(BETA*GAMMA))**3.41
      GO TO 111
C
C AR IS THE QUANTITY SMALL A, FROM BLUNCK AND WESTPHAL,
C   MULTIPLIED BY R, THE TARGET THICKNESS IN CENTIMETERS.
C
  111 AR=0.154*Z*T/A/BETA/BETA
C
C COMPUTE BS2, THE SMALL B SQUARED FROM THE BLUNCK AND
C   LEISEGANG PAPER.
C
      BS2=3.*SB/(Z*AR)
C
```

```
C VAR1, VAR2, AND VAR3 ARE CONVENIENCE STORAGE LOCATIONS
C   USED TO STORE COMPUTED PORTIONS OF STERNHEIMER'S AVERAGE
C   ENERGY LOSS.
C
      VAR1=A1*T/BETA**2
      VAR2=B2+.43+2.*DLOG(BETA*GAMMA)
      VAR3=DLOG(EI)-BETA**2
C
C QAVE IS THE FINAL VALUE FOR THE AVERAGE ENERGY LOSS.
C
      QAVE=VAR1*(VAR2+VAR3-DELT)
      B1=DSQRT(BS2)
C
C X IS THE PORTION OF SOME TOTAL ENERGY LOSS Q DUE TO
C   IONIZATION.
C
      X=Q-X
C
C XLAMB IS THE LAMBDA VARIABLE FROM THE BLUNCK AND WESTPHAL
C   PAPER.
C
      XLAMB=(X-QAVE)/AR+DLOG(EI/AR)-1.116
      WION=0.
C
C THE VARIABLE TEST IS USED TO RESTRICT OUTPUT TO NUMBERS
C   OF USEFUL MAGNITUDE.
C
      TEST=XLAMB**2/(B1*B1+3.24)
      IF(TEST.GT.138.)GOTO112
C
C COEFF ARE THE COEFFICIENTS FOR EACH OF THE FOUR GAUSSIAN
C   CURVES BLUNCK AND WESTPHAL USE TO FIT THE LANDAU DISTRI-
C   BUTION.  AN ADDITIONAL CONSTANT HAS BEEN MULTIPLIED INTO
C   EACH FOR CONVENIENCE IN RUNNING THE PROGRAM.
C
      COEFF1=(0.174*1.8)/DSQRT(B1*B1+1.8*1.8) *.1D7
      COEFF2=(0.358*2.0)/DSQRT(B1*B1+2.0*2.0)*.1D7
      COEFF3=(0.019*3.0)/DSQRT(B1*B1+3.0*3.0)*.1D7
      COEFF4=(0.007*5.0)/DSQRT(B1*B1+5.0*5.0)*.1D7
C
C GAUS ARE THE B-W GAUSSIAN CURVES INCLUDING COEFFICIENTS.
C
      GAUS1=COEFF1*DEXP(-(XLAMB-0.0)**2/(B1*B1+1.8*1.8))
      GAUS2=COEFF2*DEXP(-(XLAMB-3.0)**2/(B1*B1+2.0*2.0))
      GAUS3=COEFF3*DEXP(-(XLAMB-6.5)**2/(B1*B1+3.0*3.0))
      GAUS4=COEFF4*DEXP(-(XLAMB-11.0)**2/(B1*B1+5.0*5.0))
C
C CORINT IS AN EMPERICALLY DERIVED CORRECTION FACTOR TO COM-
C   PENSATE FOR THE FACT THAT THE DISTRIBUTION FUNCTION CAN-
C   NOT BE INTEGRATED EXACTLY AS THE RADIATION LOSS DISTRI-
C   BUTION BECOMES INFINITE AS ITS VARIABLE (ENERGY LOSS)
C   APPROACHES ZERO.
C
      CORINT=1.26*(1.-.01827*T**3.03)
      GAUS1=GAUS1*CORINT
C
C WION IS THE SUM OF GAUSSIAN CURVES REPRESENTING THE ENERGY
C   DISTRIBUTION DUE TO IONIZATION LOSSES.
C
      WION=GAUS1+GAUS2+GAUS3+GAUS4
  112 RETURN
      END
```

```
      REAL FUNCTION WRAD*8(X,EI,T,Z,A,Q)
C
C PURPOSE: THIS FUNCTION CALCULATES THAT PART OF THE ENERGY
C    DISTRIBUTION OF AN ELECTRON DUE TO LOSS OF ENERGY BY
C    RADIATION WHILE PASSING THROUGH AN ABSORBER.
C
      IMPLICIT REAL*8(A-H,O-Z)
C
C U IS AN INTERMEDIATE STORAGE LOCATION USED IN COMPUTING
C    ALPHA.
C
      U=183.0/Z**(1./3.0)
C
C COMPUTE VALUE OF ALPHA*R FOR TARGET THICKNESS, ATOMIC
C    NUMBER AND ATOMIC WEIGHT OF EXPERIMENTAL ABSORBER.  R IS
C    THE TARGET THICKNESS EXPRESSED IN CENTIMETERS.
C
      ALPHR=0.0014*T*Z*Z/A*(4.0/3.0*DLOG(U)+1.0/9.0)
C
C COMPUTE VALUE FOR B, A NORMALIZING CONSTANT.
C
      B=1./DGAMMA(ALPHR+1.)
C
C COMPUTE WRAD, THE NUMBER OF COUNTS EXPECTED AS A RESULT OF
C    RADIATION ENERGY LOSSES.  X REPRESENTS THAT PORTION OF
C    SOME TOTAL ENERGY LOSS WHICH IS NOT LOST BY IONIZATION.
C
      WRAD=(B*ALPHR*(X**ALPHR)/(EI**ALPHR))/X
      RETURN
      END




      REAL FUNCTION BEAM*8(EI,HW,X)
C
C PURPOSE: THIS FUNCTION REPLICATES THE DISTRIBUTION OF
C    BEAM ENERGY AS A SIMPLE GAUSSIAN CURVE BASED ON THE
C    EXPERIMENTALLY OBSERVED HALFWIDTH AND IS LOCATED
C    RELATIVE TO THE BEAM ENERGY BY THE COMPUTED AVERAGE
C    RECOIL LOSS.
C
      IMPLICIT REAL*8(A-H,O-Z)
      Y=2.
      ALFA=4.*DLOG(Y  )/(HW*HW)
      BEAM=DEXP(-((X-EI)**2)*ALFA)
      RETURN
      END




      REAL FUNCTION FCT*8(X,Z,A,T,EI,Q)
C
C PURPOSE: THIS FUNCTION MULTIPLICATIVELY JOINS TOGETHER THE
C    PREDICTION OF ENERGY LOSS DUE TO IONIZATION AND THE LOSS
C    DUE TO RADIATION.
C
      IMPLICIT REAL*8(A-H,O-Z)
      FCT=WRAD(X,EI,T,Z,A,Q )*AION(X,EI,T,Z,A,Q )
      RETURN
      END
```

```
      SUBROUTINE GRAPH(THX,THY,EXX,EXY,T1,T2,T3,T4,HW,EI,T,
     1CORR,CTSNOR,QP)
C
C PURPOSE: THIS SUBROUTINE PLOTS THE RESULTS OF THEORY CAL-
C   CULATIONS AND EXPERIMENTAL RESULTS.
C
      IMPLICIT REAL*8(A-H,O-Z)
      REAL*8 TITLEX(1)
      DATA TITLEX/'MEV      '/
      REAL*8 TITLEY(3)
      DATA TITLEY/'NORMALIZED COUNTS        '/
      REAL*8 TITLEO(2)
      DATA TITLEO/'OPPEDAHL BOX O  '/
      DIMENSION T1(4),T2(4),T3(4),T4(4),THX(300),THY(300),
     1EXX(200),EXY(200),CTSUP(200),CTSDN(200)
C
C DETERMINE SCALING FACTORS AND CHANGE THEORETICAL CURVE
C   TO PROPER LOCATION.
C
      X=8.
      Y=5.
      SIXIN=(EI-QP)*2.
      ISIXIN=SIXIN+.5
      SIXIN2=ISIXIN
      SIXIN=SIXIN2/2.
      IF(HW.EQ.0)GOTO90
      XNCR2=.5*HW
      INCR2=XNCR2+.5
      IF(INCR2.LT.1)INCR2=1
      XINCR2=INCR2
      XINCR=XINCR2/2.
      SP=SIXIN-6.*XINCR
      IF(SP.LT.0)GOTO90
      GOTO91
   90 SP=0
      INCR=(EI-1.5*T)/6.+.5
      XINCR=INCR
   91 N=0
      I=0
   20 I=I+1
      IF(EXX(I).GT.1.) GOTO21
      GOTO22
   21 N=N+1
      GOTO 20
   22 IF(N.EQ.0)GOTO100
      DO 23 J=1,N
      EXX(J)=(EXX(J)-SP)/XINCR+CORR/XINCR
      IF(J.EQ.N)GOTO23
   23 CONTINUE
  100 I=0
      M=0
   30 I=I+1
      IF(THX(I).GT.1.) GOTO 31
      GOTO32
   31 M=M+1
      GOTO30
   32 DO 33 J=1,M
      THX(J)=(THX(J)-SP)/XINCR
      IF(J.EQ.M)GOTO33
      IF(THY(J+1).GT.THY(J))THYMAX=THY(J+1)
   33 CONTINUE
      IF(N.EQ.0)GOTO101
      SCALE=4.
      IF(T.GT.4.8) SCALE=3.
      DO 40 J=1,N
      EXY(J)=EXY(J)/CTSNOR*SCALE
   40 CONTINUE
  101 DO 50 J=1,M
      SCALE=4.
      IF(T.GT.4.8) SCALE=3.
```

```
      THY(J)=THY(J)/THYMAX*SCALE
   50 CONTINUE
C
C SORT EXX AND ELIMINATE VALUES OFF GRAPH.
C
      IF(N.EQ.0)GOTO102
      K=N-1
      DO 60 I=1,K
      IP1=I+1
      DO 60 J=IP1,N
      IF(EXX(I).LE.EXX(J)) GOTO 60
      TEMP=EXX(I)
      TEM=EXY(I)
      EXX(I)=EXX(J)
      EXY(I)=EXY(J)
      EXX(J)=TEMP
      EXY(J)=TEM
   60 CONTINUE
      J=0
      KK=0
      K=N
      DO 61 I=1,K
      IF(KK.EQ.1)GOTO61
      IF(EXX(I).LT.0)GOTO61
      J=J+1
      N=J
      EXX(J)=EXX(I)
      EXY(J)=EXY(I)
      IF(EXX(J).GT.X)GOTO62
      GOTO 61
   62 N=J-1
      KK=1
   61 CONTINUE
  102 KK=0
      J=0
      K=M
      DO 71 I=1,K
      IF(KK.EQ.1)GOTO71
      IF(THX(I).LT.0)GOTO71
      J=J+1
      M=J
      THX(J)=THX(I)
      THY(J)=THY(I)
      IF(THX(I).GT.X)GOTO72
      GOTO71
   72 M=J-1
      KK=1
   71 CONTINUE
C
C DETERMINE ERROR BAR MAGNITUDE.
C
      IF(N.EQ.0)GOTO103
      DO 700 I=1,N
      CTSDN(I)=EXY(I)-DSQRT(EXY(I)*200.)/200.
      CTSUP(I)=EXY(I)+DSQRT(EXY(I)*200.)/200.
  700 CONTINUE
C
C INITIALIZE PLOT AND WRITE IDENTIFICATION.
C
  103 CALL PLOTS
      CALL SYMBOL(0,0,.28,TITLE0,0,16)
      CALL PLOT(0,2.,-3)
C
C DRAW OUTLINE OF GRAPH.
C
      Z=0
      CALL PLOT(Z,Y,2)
      CALL PLOT(X,Y,2)
      CALL PLOT(X,Z,2)
      CALL PLOT(Z,Z,2)
C
C DRAW OUTLINE OF TITLE BOX.
```

```
      B1=.4
      B2=4.4
      B3=3.54
      B4=4.6
      B5=B1+.1
      B6=B3+.1
      CALL PLOT(B1,B3,3)
      CALL PLOT(B2,B3,2)
      CALL PLOT(B2,B4,2)
      CALL PLOT(B1,B4,2)
      CALL PLOT(B1,B3,2)
      CALL SYMBOL(B5,B6,.14,      T1,0.0,32)
      B5=B5+.24
      CALL NUMBER(B5,B6,.14,T,0.0,3)
      B5=B5+1.32
      B6=B6+.1
      EXP=2.
      CALL NUMBER(B5,B6,.07,EXP,0.0,-1)
      B5=B5+1.20
      B6=B6-.1
      CALL NUMBER(B5,B6,.14,FI,0.0,2)
      B5=B5-2.76
      B6=B6+.24
      CALL SYMBOL(B5,B6,.14,      T2,0.0,32)
      IF(N.EQ.0)GOTO701
      B6=B6+.07
      B5=B5+.82
      B7=B5+.58
      CALL PLOT (B5,B6,3)
      CALL PLOT (B7,B6,2)
      B6=B6-.07
      B5=B5-.82
  701 B6=B6+.24
      CALL SYMBOL(B5,B6,.14,      T3,0.0,32)
      B6=B6+.24
      CALL SYMBOL(B5,B6,.14,      T4,0.0,32)
C
C PLOT TIC MARKS.
C
      G=.1
      H=Y-.1
 1570 CALL PLOT(G,Y,3)
      CALL PLOT(G,H,2)
      G=G+.1
      IF (G.LE.X)GO TO 1570
      G=X-.1
      H=.1
 1580 CALL PLOT(G,H,3)
      CALL PLOT(G,0.,2)
      G=G-.1
      IF(G.GT.0.)GO TO 1580
      G=1.
      H=.2
 1670 CALL PLOT(G,H,3)
      CALL PLOT(G,0,2)
      G=G+1.
      IF(G.LT.X) GO TO 1670
      H=Y-.2
 1680 CALL PLOT(G,H,3)
      CALL PLOT(G,Y,2)
      G=G-1.
      IF(G.GT.0.) GO TO 1680
      G=.1
      H=Y-.1
 1571 CALL PLOT(G,H,3)
      CALL PLOT(0.,H,2)
      H=H-.1
      IF(H.GT.0.) GO TO 1571
      G=X-.1
      H=.1
 1581 CALL PLOT(G,H,3)
      CALL PLOT(X,H,2)
```

```
      H=H+.1
      IF(H.LT.Y) GO TO 1581
      G=X-.2
      H=Y-1.
 1671 CALL PLOT(G,H,3)
      CALL PLOT(X,H,2)
      H=H-1.
      IF(H.GT.0) GO TO 1671
      G=.2
      H=1.
 1681 CALL PLOT(G,H,3)
      CALL PLOT(0,H,2)
      H=H+1.
      IF(H.LT.Y) GO TO 1681
C
C LABEL AXIS.
C
      CALL SYMBOL(3.5,-.6,.14,TITLEX,0,4)
      CALL SYMBOL(-.25,1.55,.14,TITLEY,90.,24)
C
C NUMBER ENERGY AXIS.
C
 1050 G=-.28
      H=-.32
      FLO=SP
 1060 CALL NUMBER(G,H,.14,FLO,0,2)
      G=G+1.
      IF(G.GT.X) GO TO 1070
      FLO=FLO+XINCR
      GO TO 1060
C
C PLOT EXPERIMENTAL DATA.
C
 1070 IF(N.EQ.0)GOTO104
      CALL LINE(EXX.EXY,N,2,-6)
C
C PLCT ERROR FLAGS.
C
      DO 1010  I=1,N
      ES1=EXX(I)-.05
      ES2=EXX(I)+.05
      CALL PLOT(ES1,CTSUP(I),3)
      CALL PLOT(ES2,CTSUP(I),2)
      CALL PLOT(EXX(I),CTSUP(I),3)
      CALL PLOT(EXX(I),CTSDN(I),2)
      CALL PLOT(ES1,CTSDN(I),3)
      CALL PLOT(ES2,CTSDN(I),2)
 1010 CONTINUE
C
C PLCT THEORY CURVE.
C
  104 CALL LINE(THX,THY,M,2,1)
C
C FINALIZE PLOT.
C
      CALL PLOT(0.,8.,-3)
      CALL PLOTE
      RETURN
      END
```

BIBLIOGRAPHY

1. Landau, L., Journal of Physics, USSR, vol. 8, p. 201, 1944.
2. Williams, E. J., Proc. Roy. Soc., London, vol. 125, p. 420, 1929.
3. Blunck, O., and K. Westphal, Zeitschrift fur Physik, vol. 130, p. 641, 1951.
4. Bumiller, F. A., F. R. Buskirk, J. N. Dyer, and R. D. Miller, Zeitschrift fur Physik, vol. 223, p. 415, 1969.
5. Miller, R. D., Energy Loss of High Energy Electrons in Aluminum, Master's Thesis, Naval Postgraduate School, 1968.
6. Goodwin, J. C., Energy Loss of High Energy Electrons in Aluminum and Copper, Master's Thesis, Naval Postgraduate School, 1968.
7. Bumiller, F. A., F. R. Buskirk, J. N. Dyer, Zeitschrift fur Physik, vol. 234, p. 185, 1970.
8. DeLeuil, W. R., and J. B. Raynis, Energy Loss of High Energy Electrons in Aluminum, Copper, and Lead, Master's Thesis, Naval Postgraduate School, 1969.
9. Mosbrooker, M. L., and D. L. Sandquist, Energy Loss of High Energy Electrons in Tin, Lead, and Gadolinium, Master's Thesis, Naval Postgraduate School, 1970.
10. Blunck, O., and S. Leisegang, Zeitschrift fur Physik, vol. 128, p. 500, 1950.
11. Sternheimer, R. M., Physical Review, vol. 88, p. 851, 1952.
12. Sternheimer, R. M., Physical Review, vol. 91, p. 156, 1953.
13. Sternheimer, R. M., Physical Review, vol. 109, p. 511, 1956.
14. Kenaston, G. W., C. T. Luke, Jr., and W. C. Sones, A Multi-channel Electron Detection System for Use in a Stabilized Magnetic Spectrometer, Master's Thesis, Naval Postgraduate School, 1965.
15. Jackson, J. D., Classical Electrodynamics, p. 456-459, Wiley, 1962.

INITIAL DISTRIBUTION LIST

		No. Copies
1.	Defense Documentation Center Cameron Station Alexandria, Virginia 22314	2
2.	Library, Code 0212 Naval Postgraduate School Monterey, California 93940	2
3.	Professor John N. Dyer Department of Physics, Code 61 Naval Postgraduate School Monterey, California 93940	10
4.	Commander Phillip E. Oppedahl, Class 50 Armed Forces Staff College Norfolk, Virginia 23511	1
5.	Captain William F. Barry U.S. Army Engineer School, EOAC 72-1 Fort Belvoir, Virginia 22060	1
6.	Chief of Personnel Operations Attn: OPD - OPEN Department of the Army - STOP 106 Washington, D. C. 20315	1

DOCUMENT CONTROL DATA - R & D

(Security classification of title, body of abstract and indexing annotation must be entered when the overall report is classified)

1. ORIGINATING ACTIVITY *(Corporate author)* Naval Postgraduate School Monterey, California 93940	2a. REPORT SECURITY CLASSIFICATION Unclassified 2b. GROUP

3. REPORT TITLE

Energy Loss of High Energy Electrons in Various Metals: Comparison of Theory and Experiment

4. DESCRIPTIVE NOTES *(Type of report and inclusive dates)*

Master's Thesis; June 1971

5. AUTHOR(S) *(First name, middle initial, last name)*

William F. Barry
Phillip E. Oppedahl

6. REPORT DATE June 1971	7a. TOTAL NO. OF PAGES 71	7b. NO. OF REFS 15
8a. CONTRACT OR GRANT NO. b. PROJECT NO. c. d.	9a. ORIGINATOR'S REPORT NUMBER(S) 9b. OTHER REPORT NO(S) *(Any other numbers that may be assigned this report)*	

10. DISTRIBUTION STATEMENT

Approved for public release; distribution unlimited.

11. SUPPLEMENTARY NOTES	12. SPONSORING MILITARY ACTIVITY Naval Postgraduate School Monterey, California 93940

13. ABSTRACT

A comparison of data from all previous energy loss experiments performed at the Naval Postgraduate School with new theoretical predictions is presented in this thesis. In addition, the data have been extended to include beryllium. With this extension, experiments have now been conducted on materials ranging in atomic number from 4 to 82. Agreement between experiment and theory is excellent for the most probable energy loss. However, theoretical values for the half-widths of the energy loss distributions generally are small compared to experiment for thicknesses less than 5 g/cm^2 and large for thicknesses greater than 5 g/cm^2. These experiments were conducted in the energy range from 50 to 100 MeV, with absorber thicknesses from 0.7 to 5.9 g/cm^2. These effects were found to be independent of atomic number or incident energy.

KEY WORDS	LINK A		LINK B		LINK C	
	ROLE	WT	ROLE	WT	ROLE	WT
Aluminum, Energy Loss of Electrons in						
Beryllium, Energy Loss of Electrons in						
Copper, Energy Loss of Electrons in						
Gadolinium, Energy Loss of Electrons in						
Lead, Energy Loss of Electrons in						
Tin, Energy Loss of Electrons in						
Electrons, Energy Loss in Various Metals						
Energy Loss of Electrons in Various Metals						
Linear Accelerator (LINAC)						

128577

Thesis
B24223 Barry
c.1

Energy loss of high energy electrons in various metals: comparison of theory and experiments.

128577

Thesis
B24223 Barry
c.1

Energy loss of high energy electrons in various metals: comparison of theory and experiments.

thesB24223
Energy loss of high energy electrons in
3 2768 002 01478 9
DUDLEY KNOX LIBRARY